

2006

TMEM27: A Cleaved and Shed Plasma Membrane Protein That Stimulates Pancreatic Beta Cell Proliferation

Pinar Akpınar

Follow this and additional works at: http://digitalcommons.rockefeller.edu/student_theses_and_dissertations

 Part of the [Life Sciences Commons](#)

Recommended Citation

Akpınar, Pinar, "TMEM27: A Cleaved and Shed Plasma Membrane Protein That Stimulates Pancreatic Beta Cell Proliferation" (2006). *Student Theses and Dissertations*. Paper 2.



TMEM27: A CLEAVED AND SHED PLASMA MEMBRANE PROTEIN
THAT STIMULATES PANCREATIC BETA CELL PROLIFERATION

A Thesis Presented to the Faculty of
The Rockefeller University
In Partial Fulfillment of the Requirements for
the degree of Doctor of Philosophy

by

Pinar Akpınar

June 2006

ABSTRACT

The signals and the molecular mechanisms that regulate the replication of terminally differentiated β cells are unclear. In this thesis I report the identification of a gene encoding transmembrane protein 27 (TMEM27) in pancreatic β cells. Expression of Tmem27 is reduced in *Tcf1*^{-/-} mice, which exhibit defects in proliferation, and is increased in islets of *ob/ob*, *db/db* and *aP2-Srebp-1c* transgenic mice with marked hypertrophy of the endocrine pancreas. Tmem27 is expressed in hormone positive cells at early stages of pancreas development and becomes restricted to pancreatic β cells in the mature pancreas. Biochemical characterization revealed that the Tmem27 exists as a dimer and that its extracellular domain is glycosylated, cleaved and shed from the plasma membrane. The cleavage process of Tmem27 is β cell-specific and does not occur in other cell types. Overexpression of full-length Tmem27, but not the truncated or soluble protein, in MIN6 cells leads to increased thymidine incorporation, whereas silencing of Tmem27 using RNAi results in a reduction of cell replication. Furthermore, transgenic mice with increased expression of Tmem27 in pancreatic β cells exhibit increased β cell mass compared to their control littermates. The following results identify a novel pancreatic β cell-shed protein that regulates cell growth of pancreatic islets.

ACKNOWLEDGEMENTS

I have spent a most enjoyable and productive four and a half years at Rockefeller and I would like to thank a number of people whose support I have greatly appreciated.

First and foremost, I would like to thank Markus Stoffel for being a wonderful mentor. I very much appreciated his penchant for science and I would like to thank him for teaching me how to ask useful questions in scientific research.

I have especially enjoyed working on my Ph.D. in the Stoffel lab as I had wonderful friends and colleagues who made work a fun and pleasant place to be everyday. I would especially like to acknowledge Vivian Lee, Jenni Lowe, Latif Rachdi, Jan Kruetzfeldt, Christian Wolfrum, and Satoru Kuwajima for their friendship and all the help they have offered me over the years.

I have made many valuable friendships at Rockefeller and there are too many names to list here. However, I have to single out Francisco Lopez de Saro for always finding solutions to my random scientific problems and Bahar Taneri for always taking the time to talk.

I would not be where I am today if it had not been for my parents, Guner and Ismail Akpinar. Their vision and drive for me and my sister have been most instrumental in our lives and I owe my success to them.

Lastly and most importantly, I would like to thank James, my closest friend of all, for his constant support, love, and for being a joy to come home to everyday.

TABLE OF CONTENTS

INTRODUCTION

1.1	Introduction to diabetes mellitus	1
1.2	Regulation of islet mass	2
1.3	Overview of pancreas development	5
1.4	Network of transcription factor regulate β cell development and function	7
1.5	Maturity-onset diabetes of the young (MODY)	11
1.6	Identification of a Tcf1 target gene involved in β cell growth	18

RESULTS

2.1	Tmem27 expression is regulated by Tcf1	20
2.2	Pdx-1 binds to a conserved site in Tmem27 promoter	23
2.3	Tmem27 is regulated during pancreas development	24
2.4	Tmem27 is an N-linked glycoprotein and forms dimers in vivo	26
2.5	Tmem27 is cleaved and shed from pancreatic β cells	28
2.6	Tmem27 is a constitutively shed plasma membrane protein	33
2.7	Search for a cleavage site and protease	38
2.8	Tmem27 influences insulin secretion	46
2.9	Increased expression of Tmem27 in mouse models with islet hypertrophy and enhanced β cell replication in vitro	49

2.10 Transgenic mice overexpressing Tmem27 in pancreatic islets	57
exhibit hypertrophy	

DISCUSSION

3.1 Tcf1 regulates expression of Tmem27	63
3.2 Expression of Tmem27 in embryonic pancreas development	64
3.3 Ectodomain shedding of Tmem27	65
3.4 Tmem27 influences insulin secretion	69
3.5 Tmem27 stimulated β cell growth in vivo	70
3.6 Conclusion	76

EXPERIMENTAL PROCEDURES

4.1 Experimental Procedures	78
Experimental animals	78
Vectors	78
Antibodies	79
Cell culture	79
Transient transfections and luciferase assay	80
Crosslinking of proteins in cell lysates	80
Inhibition and enzymatic cleavage of N-glycosylation	81
Electrophoretic mobility shift assay (EMSA)	81
Whole cell extract preparation	82

Pulse-Chase experiment	83
In vitro insulin secretion and hormone measurements	84
Pancreatic islet and RNA isolation	84
Islet morphometry	85
RT-PCR	85
Immunoblotting and immunohistochemistry	86
Electron microscopy studies	87
Thymidine incorporation studies	88
RNA interference	89
Generation of adenovirus	89
Generation of RIP-Tmem27 mice	90
Bacterial protein production	90
S2 cell protein production	91
PCR-directed mutagenesis	92
Protease inhibitors	92
Statistical analysis	93
REFERENCES	94

LIST OF FIGURES

	Page
Figure 1: Dorsal and ventral pancreatic buds in the embryo	6
Figure 2: Branching morphogenesis of embryonic pancreas	7
Figure 3: Transcription factors in endocrine cell specification	9
Figure 4: Tmem27 expression in Tcf1 ^{-/-} islets	20
Figure 5: Promoter sequence for human and mouse Tmem27	21
Figure 6: Transcription activation assays	22
Figure 7: Tcf1 binds to Tmem27 promoter sequence in vitro	22
Figure 8: Tcf1 binds to Tmem27 promoter in vivo	23
Figure 9: Transcriptional activation assay with Pdx-1	24
Figure 10: Tmem27 is expressed in developing mouse pancreas	25
Figure 11: Tmem27 is an N-glycosylated protein	27
Figure 12: Tmem27 forms dimmers in vivo	27
Figure 13: Schematic drawing of Tmem27 protein	28
Figure 14: Tmem27 is detected as two bands on western blots	29
Figure 15: Only β cel lines release soluble Tmem27	30
Figure 16: Mouse islets release soluble Tmem27	30
Figure 17: Removal of N-glycosylation from soluble Tmem27	31
Figure 18: si-Tmem27 treated MIN6 cells shed less soluble protein	31

Figure 19: HA-tagged Tmem27 is shed from MIN6 cells	32
Figure 20: Tmem27 is a plasma membrane protein	33
Figure 21: Subcellular fractionation of MIN6 cells	34
Figure 22: Immunodetection of Tmem27 with electron microscopy	35
Figure 23: Tmem27 is not released with insulin in islets	36
Figure 24: Tmem27 release is not glucose stimulated in MIN6 cells	36
Figure 25: Tmem27 is constitutively released from MIN6 cells	37
Figure 26: Immunoprecipitation of Tmem27 from MIN6 supernatant	38
Figure 27: Tmem27 is not cleaved by prohormone convertases	40
Figure 28: Primary hepatocytes do not shed Tmem27	41
Figure 29: Tmem27 is not cleaved by a soluble protease	42
Figure 30: PMA induces Tmem27 shedding only from β cells	43
Figure 31: Various protease inhibitors do not affect Tmem27 release	43
Figure 32: BB94 inhibits PMA stimulated Tmem27 shedding	44
Figure 33: ADAM9 is not involved in Tmem27 cleavage	45
Figure 34: Tmem27 overexpression inhibits insulin secretion	46
Figure 35: Reduced Tmem27 expression leads to increased insulin secretion	47
Figure 36: Tmem27 does not affect insulin content	47
Figure 37: Tmem27 does not interact with SNARE complex proteins	48
Figure 38: Tmem27 does not co-localize with VAMP2 or syntaxin	48

Figure 39: Tmem27 expression is increased in islet hypertrophy	49
Figure 40: Ob/ob islets shed increased amount of soluble Tmem27	50
Figure 41: Tmem27 expression in BKS-Lepr/J mouse	51
Figure 42: Tmem27 regulates cell proliferation	52
Figure 43: Tmem27 expression has no effect on apoptosis	53
Figure 44: Expression of truncated Tmem27	54
Figure 45: Truncated Tmem27 does not increase proliferation	54
Figure 46: Truncated Tmem27 conserves localization and dimerization	55
Figure 47: Co-culture does not affect cell proliferation	55
Figure 48: Conditioned media does not affect cell proliferation	56
Figure 49: Increased Tmem27 protein levels in transgenic mice	57
Figure 50: Comparison of pancreata from transgenic and wildtype mice	58
Figure 51: Islet hypertrophy in transgenic mice	58
Figure 52: No difference in non- β -cell mass in transgenic mice	59
Figure 53: Insulin content of pancreas is increased in transgenic mice	59
Figure 54: No difference in ITT between transgenic and control mice	59
Figure 55: No difference in plasma hormone levels of transgenic mice	60
Figure 56: Transgenic and control mice have similar IPGTT	61
Figure 57: Transgenic and control mice exhibit similar GSIS	61
Figure 58: Transgenic mice respond better to high fat diet	62

LIST OF TABLES

	Page
Table 1: Transcription factors important in endocrine cell development	11
Table 2: Screen with protease inhibitors	44

1.1 Introduction to diabetes mellitus

The number of people with diabetes has been rising at a disconcerting rate worldwide with significant increases in the last two decades. As of 2001, an estimated 150 million people globally had diabetes and this number is expected to reach 220 million people by 2010 and 300 million by 2025 (Zimmet et al., 2001). Diabetes is a heterogeneous group of disorders characterized by high fasting blood glucose levels (ADA Report, 2001). There are two major forms of diabetes. Type 1 diabetes, also known as juvenile-onset diabetes, occurs as a result of an autoimmune mediated destruction of the insulin producing β cells of the pancreas. The more prevalent type 2 diabetes accounts for more than 90% of people with diabetes and is a complex disease that develops as a result of both genetic and environmental factors. Diabetics of both types develop serious micro- and macrovascular complications that affect the kidney, heart, extremities, eyes, and lead to renal failure, heart attack, gangrene, stroke, and blindness. Thus diabetes already imposes a considerable burden on health-care systems and will develop into a major international public health threat in the future.

Type 2 diabetes may develop as a result of various defects in diverse molecular pathways. The precise regulation of plasma glucose levels requires a balance between the function of pancreatic β cells and the responsiveness of

metabolic tissues such as muscle, liver, and fat. Genetic disposition as well as obesity and sedentary lifestyle are contributing factors to type 2 diabetes, which involves insulin resistance and/or dysfunctional β cells. Hence, defects in β cell growth and function play a central role in the pathophysiology of both type 1 and 2 diabetes.

The pancreas is derived from the endoderm and consists of three distinct cell populations called the endocrine, acinar, and ductal cells. The acinar cells make up the exocrine pancreas that secrete digestive enzymes into the intestine. The endocrine cells are the major constituents of islets that secrete hormones into the blood stream (Slack, 1995). Pancreatic islets are comprised mainly of β cells (80%) that secrete insulin and to a lesser extent of α cells (10-15%) that secrete glucagon, δ cells that secrete somatostatin, PP cells that secrete pancreatic polypeptide and ϵ cells that express ghrelin (Prado et al, 2004).

1.2 Regulation of islet mass

Endocrine hormones tightly regulate energy metabolism in the body and islet mass is dynamic and adaptable in response to metabolic demand. In a number of metabolic states such as growth, pregnancy, insulin resistance due to obesity and in various injury models, islet mass seems capable of compensating both functionally and morphologically. In fact, only 15-20% of people with

obesity or severe insulin resistance become diabetic and most people are able to maintain normoglycemia due to β cell compensation (Bonner-Weir, 2000). This phenomenon is shown in humans (Kloppel, 1985) and in experimental rodent models. In Zucker fa/fa rat, a nondiabetic animal model of obesity, β cell mass increases 4-fold compared with lean controls (Pick, 1998). During pregnancy, β cell mass adjusts considerably and it has been shown in the rat that β cell mass increases by about 50% due to increased β cell proliferation induced by placental lactogen and increased cell volume as a functional adaptation. β cell mass also continues to increase during postnatal growth and in rodents it is linearly correlated with body weight (Bonner-Weir, 2000). β cells are also capable of decreasing their mass when it is necessary. After pregnancy, a rapid decrease of the β cell mass occurs in postpartum rats (Marynissen et al., 1983). This is accompanied by decreased β cell replication and β cell size, and by an increased frequency of apoptosis (Scaglia et al., 1995).

The mass of β cells is governed by the balance of β cell growth (replication) and β cell death (apoptosis) (Bonner-Weir, 2000; Lingohr et al., 2002; Butler et al., 2003; Flier et al., 2001). However, the identity of the factors that control β cell mass remains elusive. In the adult organism, maintenance of β cell mass involves replication of preexisting cells (Dor et al., 2004) and recent evidence substantiates that regeneration of islets even after injury does not

display recapitulation of neogenesis present during development (Lee et al., 2006). Thus, understanding how β cell mass is regulated is important to design rational approaches to prevent pancreatic β cell loss and to expand β cells for transplantation in type 1 diabetes.

During development, β cells are generated from a population of pancreatic progenitor cells (Edlund, 2002; Wilson et al., 2003). The β cells that differentiate from progenitor cells are postmitotic, and direct lineage tracing studies indicate that a population of progenitor cells persists throughout embryogenesis to allow the differentiation of new β cells (Dor et al., 2004; Gu et al., 2002; Gradwohl et al., 2000). In the neonatal period new β cells are formed by replication of differentiated β cells, which results in a massive increase in β cell mass (Finegood et al., 1995; Svenstrup et al., 2002). In adulthood there is little increase in the β cell number except in conditions of increased demand and the growth stimulatory signals in pathological insulin resistant states are not well understood.

Several mouse models of insulin resistance and diabetes, such as the *ob/ob* and *db/db* mice or mutant mice created by inactivation of the gene for insulin receptor substrate-1 (*Irs-1*) or double heterozygous knockout of the insulin receptor and *Irs-1*, exhibit marked islet hyperplasia (Bock et al., 2003; Tomita et al., 1992; Gapp et al., 1983; Kulkarni et al., 2004 and Kahn, 2003). In contrast, loss

of Irs-2 function leads to a dramatic reduction of β cells and diabetes (Withers et al., 1998). Glucose itself is known to stimulate β cell replication (Topp et al., 2004), however, many of the above mouse models increase their total islet mass before the onset of detectable hyperglycemia. Furthermore, in most cases the hyperplastic response bears no relationship to the level of hyperglycemia, suggesting that factors independent of glucose are likely to contribute to the islet growth.

1.3 Overview of pancreas development

Pancreas development in the mouse begins at embryonic day 9 (E9) with the emergence of dorsal and ventral epithelium buds between the stomach and duodenum (Figure 1). The molecular machinery that drives gut epithelium towards a pancreatic fate is not completely understood, however, a temporally and spatially regulated framework of transcription factors involved in the development of pancreatic tissue has been described. Pdx1 is one of the earliest expressed transcription factors in the pancreatic epithelium. It has been showed that initiation of either bud can take place without Pdx1 expression. Yet, Pdx1 expression is crucial for growth and morphogenesis of the bud epithelia (Ahlgren et al., 1996; Offield et al., 1996).

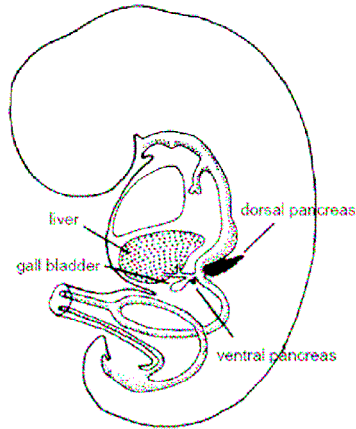


Figure 1. Location of the dorsal and ventral pancreatic buds in the developing embryo. Adapted from Slack, 1995.

The nascent buds go through remarkable growth and branching before fusing at E12.5 (Figure 2). In this early stage of pancreatic primordium expansion, there are clusters of cells that express both glucagon and insulin. The exact role of these cells is not obvious as they have been shown not to be the progenitors of hormone positive cells that make up the islet in the adult animal (Herrera, 2000), although an *ex-vivo* study using pancreatic tissue from E11 mouse embryos showed that antagonizing glucagon at this stage leads to inhibition of β cell differentiation (Prasadan et al., 2002). Between E13.5 and E15.5, there is a wave of endocrine and exocrine cell differentiation and number of insulin and glucagon positive cells as well as acinar cells expressing digestive enzymes increases dramatically. Towards the end of the fetal gestation at E18.5, development of pancreas morphology is complete as endocrine cells are organized into islet structures located among the acinar cells. Neogenesis of β cells continues through the initial days of neonatal period when the pancreatic

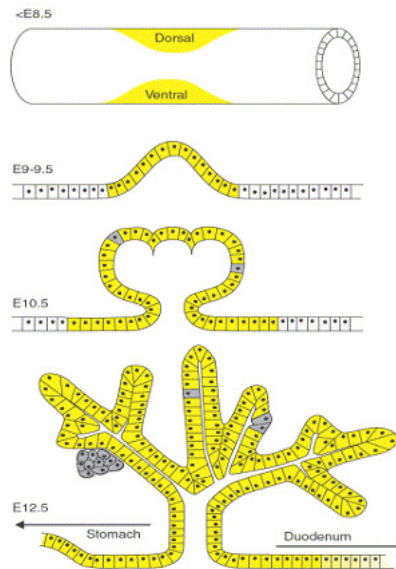


Figure 2. Branching morphogenesis in the embryonic pancreas. Yellow shading marks the cells that express Pdx-1 and the gray shading shows the differentiated early endocrine cell clusters. The diagram depicts the dorsal bud specification. Diagram is adapted from Kim and MacDonald, 2002.

islets become glucose responsive. Neogenesis can be defined as the formation of new β cells by the differentiation of previously insulin negative precursor cells and this process usually stops shortly after birth. Thereafter, β cell mass is regulated through an interplay between replication and apoptosis.

1.4 Network of transcription factors regulate β cell development and function

Several genetic interactions play a role in the early development of gut endoderm. Induction followed by patterning of pancreas involves tissue and cell-specific expression of transcription factors and is regulated by morphogens produced by mesodermal mesenchyme and vascular endothelium in a temporal and spatial fashion (Lammert et al., 2003). Development programs of the dorsal and ventral buds of the pancreas are not identical as they are two independent endodermal domains receiving distinct signals from their surrounding tissues.

Dorsal bud grows in close proximity to notochord and its development requires signals from the notochord to repress the signaling factor sonic hedgehog in the presence of Pdx-1 expression (Apelqvist et al., 1997). Ventral bud develops in close connection to the liver and bile duct epithelium. Signals that drive ventral pancreatic bud differentiation are not completely understood, however, pancreatic lineage appears to be more of a default pathway as cardiac mesoderm signaling defines liver cells and lack of this signaling leads to pancreas specification. Recent evidence implicates the homeobox protein, Hex, in control of positioning endoderm cells and specifying the ventral bud (Bort et al., 2004). Several transcription factors are critical regulators of the endodermal development and their expression in certain stages along with defined interacting partners determine differentiation programs of individual cell types (Habener et al., 2005). Transcription factors Tcf-1, Tcf-2, Foxa2, HNF4 α and Hnf6 (Onecut 1) are all expressed in the pancreatic progenitor cells that are defined by activation of Pdx-1 and Hb9. As shown in Figure 3, determination of different cell lineages in the pancreas involves activation of a cascade of transcription factors. Exocrine cell precursors express Ptf1a (p48) and endocrine cell fate is established by transient expression of the basic helix-loop-helix (bHLH) transcription factor neurogenin3 (Ngn3) (Gradwohl et al., 2000).

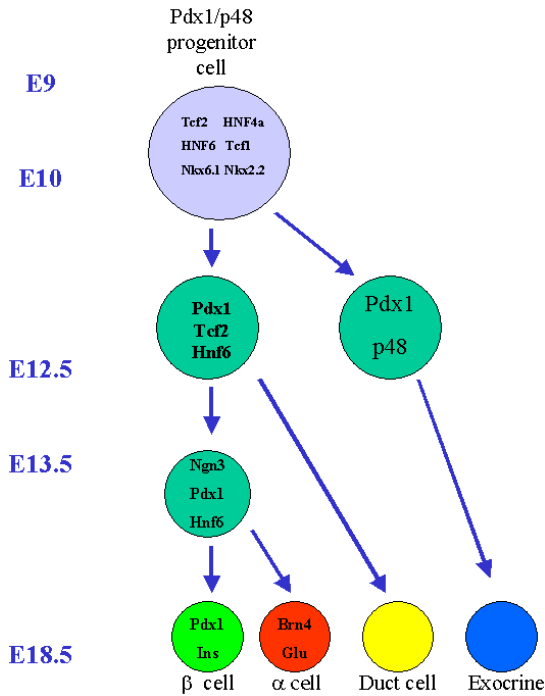


Figure 3. A cascade of transcription factor activation determines specification of cell lineages in the developing pancreas.

Phenotypic results of gene-specific knockout animals defined the expression requirements of various transcription factors (Table 1) in the development of different pancreatic cell types. NeuroD/Beta2 is expressed in precursors of both α and β cells and a terminally differentiated β cell furthermore requires activation of Pax4, MafA, Nkx2.2, and Nkx6.1. Organogenesis of the pancreas is defined by restricted expression of the above transcription factors and most of the same factors also play a role in maintaining the terminally differentiated cells. For example, Pdx-1 is widely expressed in early development of pancreas; however, in late fetal gestation its expression is gradually restricted to β cells and δ cells. The importance of transcription factors

in endocrine cell development and function has also been emphasized in humans as mutations in transcription factors TCF1, TCF2, HNF4 α , IPF-1 (Pdx-1), NEUROD/BETA2 result in a monogenic form of diabetes called the maturity-onset diabetes of the young (MODY). In the β cell, Tcf1 (MODY3), Pdx-1 (MODY4), and NeuroD (MODY6) are all shown to be direct regulators of insulin gene expression. Moreover, these transcription factors along with HNF4 α (MODY1), Tcf2 (MODY5), Hnf6 and Foxa2 exist in a transcriptional network where they regulate each other's expression. Thus the determination of the identity and the function of the β cell are achieved through expression of a unique combination of transcription factors in a specific gene regulatory network.

Table 1. Transcription factors involved in endocrine pancreas development

Transcription factor	Onset of expression	Expression in adult pancreas	Pancreas phenotype in null mutant mice	References
Foxa2	E5.5-6.5	All cells	Embryonic lethal due to lack of foregut formation	Ang et al., 1994
Hlxb9	E8		Dorsal bud fails to develop; reduction of β cells in remnant pancreas.	Li et al., 1999
Pdx-1	E8.5	β cells	Pancreas agenesis	Jonsson et al., 1994
Isl-1	E9	β , α , δ , PP cells Dorsal mesenchyme	Endocrine cells are absent.	Ahlgren et al., 1997
Hnf6	E9.5		Impaired endocrine cell differentiation; Ngn3 expression is reduced.	Jacquemin et al., 2000
Ngn3	E9-9.5		Endocrine cells and their precursors are absent.	Gradwohl et al., 2000
Beta2/NeuroD	E9.5	β , α , δ , PP cells	Islet malformation and reduced endocrine cells.	Naya et al., 1997
Pax6	E9-9.5	β , α , δ , PP cells	Islet malformation. α cells are absent.	Sander et al., 1997
Pax4	E9.5	β , δ , PP cells	β and δ cells are absent. Growth retarded mouse dies 3-5d after birth.	Sosa-Pineda et al., 1997
Nkx2.2	E9.5	β , α , PP cells	Reduced islet mass and absence of β cells. Mouse dies due to hyperglycemia.	Sussel et al., 1998
Nkx6.1	E9-9.5	β cells	β cell formation inhibited.	Sander et al., 2000

1.5 Maturity-onset diabetes of the young (MODY)

MODY is a clinically heterogeneous disorder and accounts for approximately 5-10% of patients with type 2 diabetes. MODY is characterized by autosomal dominant inheritance, an early onset usually before 25 years of age, and

development of marked hyperglycemia with a progressive impairment in insulin secretion (Shih and Stoffel, 2002). Studies using genetic linkage and candidate gene approaches have led to mutations in six genes that cause MODY in people. The MODY2 gene encodes the glycolytic enzyme glucokinase (GCK) important for glucose sensing in β cells (Frougel et al., 1993). Glucokinase catalyzes the first rate-limiting step in glycolysis and is crucial for generating the metabolic signal for insulin secretion (Matschinsky, 1990). Heterozygous mutations in the GCK gene lead to a partial deficiency of this enzyme and are associated with MODY2; homozygous mutations result in a complete deficiency of this enzyme and lead to permanent neonatal diabetes mellitus (Njolstad et al., 2001). Glucokinase-deficient mice exhibit a similar phenotype to MODY2 patients as mice that lack GCK activity die perinatally with severe hyperglycemia resembling rare forms of neonatal diabetes and heterozygous mice have elevated blood glucose levels and reduced insulin secretion. The importance of GCK activity in β cells is reinforced with further experiments in the GCK-deficient mice, which show that recovering expression of glucokinase only in β cells can rescue homozygous null mice from perinatal death (Grupe et al., 1995). Several heterozygous activating GCK mutations that cause hypoglycemia have also been reported in humans (Glaser et al., 1998; Christesen et al., 2002; Gloyn et al., 2003).

MODY4 is a rare form MODY caused by an inactivating mutation in the IPF-1/PDX-1 gene. This single nucleotide deletion (Pro63fsdelC) has been described in a patient with pancreatic agenesis (Stoffers et al., 1998). This patient inherited the mutant allele from his parents who were heterozygous for the same mutation (Stoffers et al., 1997). Heterozygous family members have early-onset diabetes (Stoffers et al., 1997b). Other PDX-1 mutations have been described to predispose carriers to diabetes and functional analysis of these variants suggested that these mutations might lead to a progressive impairment of β cell function and glucose homeostasis collectively with other risk factors (Hani et al., 1999; Macfarlane et al., 1999). Mice with targeted disruption of the Pdx-1 gene also fail to develop a pancreas and moreover, β cell-specific inactivation of Pdx-1 gene leads to a loss of β cell phenotype and diabetes (Jonsson et al., 1994; Ahlgren et al., 1998). In both humans and rodents, PDX-1 appears to be a key regulator in early pancreas formation and in maintenance of insulin expression and normoglycemia.

MODY6 is caused by mutations in the bHLH transcription factor NEUROD1/BETA2. NEUROD1 mutations so far have been described in two families with autosomal-dominant inheritance. One family showed a clinical phenotype that resembles type 2 diabetes with high fasting serum insulin levels. The second family met the criteria for MODY as three carriers in the family

displayed onset of diabetes before 25 years of age and five family members required insulin treatment consistent with β cell dysfunction and low endogenous insulin secretion (Malecki, et al., 1999). NEUROD1 regulates insulin gene expression by binding to its promoter and plays an important role in endocrine cell type determination in development. Mice deficient in NeuroD1 function have abnormal islet morphology, overt diabetes, and die after birth (Naya et al., 1997).

Transcription factors HNF4 α and Tcf1 regulate each other's expression and consequently clinical features of MODY1 and MODY3 are similar. Both MODY1 and MODY3 patients show progressive deterioration of glycemic control associated with a decrease in insulin secretion (Fajans et al., 1993). HNF4 α is a member of the nuclear receptor family of transcription factors and plays a critical role in development, cell differentiation, and metabolism of pancreatic islets as well as visceral endoderm, liver, intestine, and kidney (Stoffel and Duncan, 1997). Molecular studies indicate that HNF4 α deficiency results in impairment of insulin secretion by dysregulation of pancreatic islet gene expression and the extent of regulation by HNF4 α has recently been further substantiated using a combined chromatin immunoprecipitation with a custom promoter microarray (Odom et al., 2004). The authors discovered that over 40% of the active promoters in pancreatic islets were bound by HNF4 α including

those of genes involved in glucose metabolism and insulin secretion. In the same study, cross-regulation of TCF1 and HNF4 α has also been confirmed as they were found to occupy each other's promoters. The HNF4 α -deficient mouse is embryonic lethal, however, new data on mice generated by β cell-specific deletion of HNF4 α show that the mice exhibit impairment of glucose-stimulated insulin secretion, consistent with MODY1 phenotype, and a possible mechanism for this defect may include altered activity of K-ATP channel (Miura et al., 2006).

MODY5 transcription factor TCF2 is structurally related to TCF1. TCF1 and TCF2 are expressed in a variety of tissues and can form homodimers as well as heterodimers with each other. MODY5 patients are also characterized by reduced insulin secretion; however, their diabetic phenotype is often accompanied by progressive nondiabetic renal dysfunction (Nishigori et al., 1998). Selective deletion of the Tcf2 gene in β cells of mice manifests in impaired glucose tolerance and impaired glucose-dependent insulin release (Wang et al., 2004).

The most common form of MODY is MODY3 caused by mutations in the TCF1 gene. Depending on the racial group, MODY3 accounts for 15-73% of all described MODY patients (Frayling et al., 2001). TCF1 is a homeodomain transcription factor composed of an N-terminal dimerization domain, a POU-homeobox DNA-binding domain, and a C-terminal transactivation domain.

MODY3 phenotype in humans manifests defective glucose utilization, insulin secretion, and glucose disposal (Surmely et al., 1998). In fact, it has been reported that insulin sensitivity is actually increased in MODY3 patients making the role of β cell pathogenesis particularly central in MODY3 (Frayling et al., 2001). The most common mutation of the TCF1 gene is an insertion of C in the poly C tract around codon 291 (P291fsinsC) most likely due to slipped mispairing during DNA replication. Mutations in the TCF1 gene mainly cause diabetes through haploinsufficiency. However, it has been shown that P291fsinsC has a dominant negative effect when it is overexpressed in cell lines (Yamagata et al., 1998). Two experimental animal models of MODY3 have been generated to investigate the role of Tcf1 in β cells of the islet. Mice with targeted disruption of Tcf1 (Tcf1^{-/-}) develop a diabetic phenotype, however, also suffer from Laron dwarfism and multiple organ manifestations such as renal dysfunction with glucosuria, pathological liver tests, and hepatomegaly (Pontoglio et al., 1996; Lee et al., 1998). MODY3 carriers may display glucosuria, however, liver function is usually not affected (Stride et al., 2005). Another experimental model for MODY3 has been generated by expression of a transgene carrying the dominant negative P291fsinsC mutation in β cells of mice. These mice develop progressive hyperglycemia due to impaired glucose-stimulated insulin secretion (Hagenfeldt-Johansson et al., 2001; Yamagata et al., 2002).

Studies in islets of MODY3 models showed that Tcf1 regulates a variety of genes encoding proteins important for glucose transport, glycolysis, and mitochondrial metabolism. Specifically, Tcf1 can activate promoters of the glucose transporter type 2 (Slc2a2, Glut2), which facilitates glucose transport into β cells and L-type pyruvate kinase (PKL), which is a rate-limiting enzyme of glycolysis (Wang et al., 1998; Yamagata et al., 2002). Other genes that are regulated by Tcf1 include aldolase B, insulin, and the mitochondrial 2-oxo-glutarate dehydrogenase (OGDH) E1 subunit (Wang et al., 1998; Wang et al., 2000).

Pancreatic islets of both Tcf1^{-/-} and transgenic mice are small and irregular in shape. Transgenic mice, in particular, display abnormal islet architecture, which may be due to decreased expression of E-cadherin seen in these islets (Yamagata et al., 2002). E-cadherin is an adhesion molecule that is critical for cell-cell interaction. Both mice exhibit a progressive reduction in β cell number, proliferation rate, and pancreatic insulin content. Studies showed that Tcf1 can influence the expression of genes involved in cell proliferation and apoptosis such as IGF-1, cyclin E, p27KIP1 and Bcl-xL as well as transcription factors important for β cell development and function such as Pdx-1, HNF4 α , and NeuroD (Yang et al., 2002; Wobser et al., 2002; Shih et al., 2001). These data indicate that Tcf1 target genes are required for maintenance of normal β cell

mass; however, exact molecular pathways involved in this regulation remain elusive.

1.6 Identification of a Tcf1 target gene involved in β cell growth

In order to identify genes that are important for regulation of β cell mass, an Affymetrix microarray experiment was done to compare gene expression profiles of islets isolated from Tcf1^{-/-} mice and their wild-type littermates. This analysis led to the identification of a transcript encoding transmembrane protein 27 (Tmem27) that is markedly reduced in the islets of Tcf1^{-/-} mice.

Tmem27 is a 222 amino acid type 1a transmembrane protein that contains a signal peptide, an extracellular domain, and a transmembrane domain followed by a cytoplasmic tail. Tmem27 is highly homologous among human, rat, and mouse. Among the three species, Tmem27 shares 84.3% identity in nucleotide sequence and 81.9% homology in amino acid sequence. Tmem27 was initially termed collectrin as it has been localized to the luminal surface and cytoplasm of collecting ducts and was originally described as a kidney-specific gene that is upregulated in an injury-induced renal hypertrophy model (Zhang et al., 2001). In the only published account of Tmem27, Zhang et al. had noted the protein as a homolog of angiotensin-converting enzyme-related carboxypeptidase (ACE2) as it shares 47.8% identity with non-catalytic

extracellular, transmembrane, and cytosolic domains of ACE2. Moreover, Tmem27 expression was described during mouse kidney development. Tmem27 is detectable at E13 in the ureteric bud branches. Its expression is progressively increased in later stages of gestation extending into the neonatal periods and then is decreased in adult life (Zhang et al., 2001).

In this thesis, I describe the specific expression of Tmem27 in β cells of the endocrine pancreas. I carried out a comprehensive biochemical and functional analysis of Tmem27 and demonstrated that it is a stimulator of β cell replication *in vivo* and *in vitro*.

2.1. Tmem27 expression is regulated by Tcf1

In an attempt to identify mitogenic factors in pancreatic β cells, we compared gene expression in isolated pancreatic islets of *Tcf1*^{-/-} and wildtype littermates using Affymetrix™ oligonucleotide expression arrays. This analysis identified a gene encoding a transmembrane-spanning protein (Tmem27) that showed a 16-fold decrease in expression levels of *Tcf1*^{-/-} mice compared to controls. This result was confirmed by RT-PCR in an independent group of animals (Figure 4). To study whether Tcf1 is a direct activator of Tmem27 transcription, I analyzed the Tmem27 promoter and identified two putative Tcf1 binding sites in its regulatory region that were conserved between human and mouse (Figure 5). I cloned an 815 bp promoter region upstream of a luciferase reporter gene and co-expressed it with a Tcf1 expression vector. Transient co-transfection of Tcf1 and Tmem27 promoter led to a >7-fold activation of luciferase activity (Figure 6).

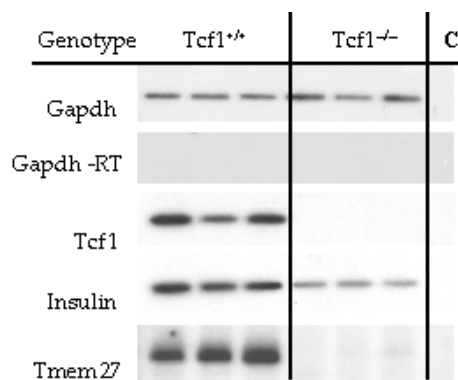


Figure 4. Tmem27 expression is decreased in the islets of *Tcf1*^{-/-} mice compared to wildtype littermate controls. Expression levels were measured with RT-PCR, GAPDH was used as a control. C: no DNA added; -RT: no reverse transcriptase added to reaction.

Human GAA AACAACTAATCTGTTTTCCAAACA
 Mouse GAAGAACCCTACTAACCTGCTTCTCAAATA

Human GGTTTCATAAATAACTGACAGGAGATGG
 Mouse GATTTTCGTAAATAACTGACAGGGGATGG

Human GCTGTTTTTATGGAAGTATTAACCCAAAT
 Mouse TTCGCTTCTATGGACGTATTAACCCAACT

Human GATGGGTGTTAAATCATTAACCTTTTTGG
 Mouse GATGGGCGTAAATATTAAACCTTTTAGA

Human TGGTGGCTCGCTTGTTT
 Mouse TGGTGGCTCGCTGATTT

Figure 5. Promoter analysis predicted two conserved Tcf binding sites in the upstream regulatory regions of human and mouse (bottom) *Tmem27* genes, at -60 and -117 base pairs relative to the transcriptional start site. Human (top) and mouse (bottom) promoter sequences are aligned and

Tcf binding sites are boxed in blue. A second site (red box) denotes a putative Pdx-1 binding site. Highlighted sequences (green) indicate positions of the mutated Tcf binding sites.

When each Tcf1 site in the *Tmem27* promoter was selectively mutated, transcriptional activation was reduced 70-80% (Figure 6). To demonstrate binding of Tcf1 to these sites in vitro I carried out electrophoretic gel mobility shift assays (EMSA) using double stranded ³²P-labeled oligonucleotides containing the respective Tcf binding sites and MIN6 cell extracts. Figure 7 shows that the probe shifted upon addition of nuclear extracts and that the site of the farnesoid X receptor promoter (Fxr)(Shih et al, 2001a). The specificity of protein binding to these sites was also determined by further shifting the DNA-Tcf1 complex using a specific anti-Tcf1 antiserum (Figure 7). I also investigated if Tcf1 directly increases the expression of *Tmem27* by performing chromatin immunoprecipitation assays (ChIP). Tcf1 bound to the binding sites in the *Tmem27* promoter of MIN6 cells and pancreatic islets but not in primary hepatocytes where *Tmem27* is not expressed (Figure 8). These data confirm the

binding could be competed by adding increasing amounts of a known binding functionality of the Tcf1 binding sites *in vivo* and demonstrate that Tcf1 is required for expression of Tmem27 in pancreatic β cells.

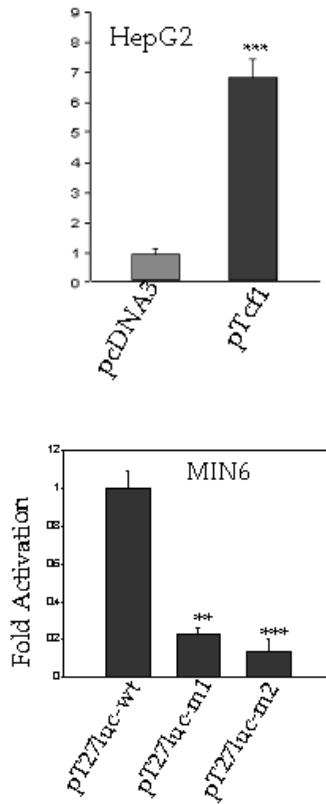


Figure 6. Transcriptional activation assays in HepG2 cells that were transfected with pcDNA3 or pTcf1, pCMV- β -galactosidase, and the luciferase reporter gene using a 815 bp Tmem27 mouse promoter (left panel). Tcf binding sites were mutated individually in the promoter sequence of the reporter vector and MIN6 cells were transfected with vectors pT27luc-wt, pT27luc-m1 or p27luc-m2. Luciferase activity was normalized to β -galactosidase activity (right panel). Each value represents the mean of eight independent experiments. *: $P < 0.05$, **: $P < 0.01$, ***: $P < 0.001$.

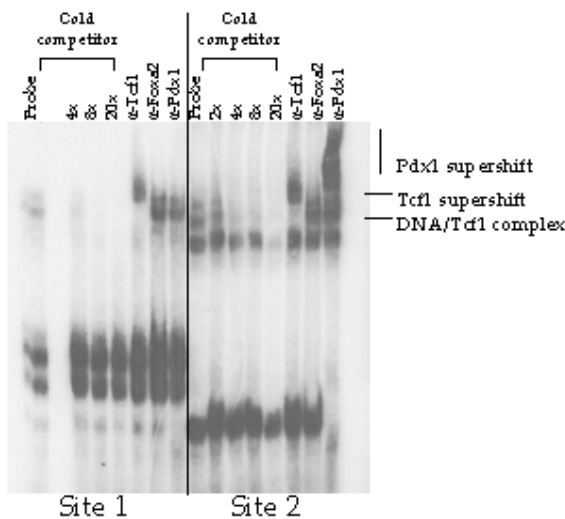


Figure 7. EMSA analysis using oligonucleotides for Tcf binding sites 1 and 2 and whole cell extracts of MIN6 cells. Competitor represents unlabeled double-stranded oligonucleotides at increasing concentrations containing Tcf1 binding site of Fxr-1 promoter (Shih et al., 2001). The signal of the free probe at the bottom of the gel was cut off.

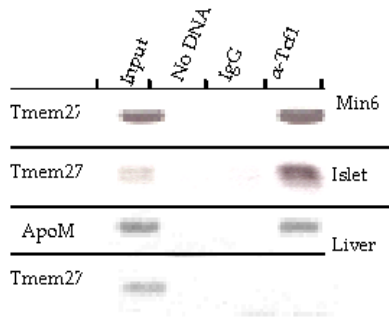


Figure 8. Chromatin immunoprecipitation assays in pancreatic islets and MIN6 cells demonstrate an *in vivo* interaction of Tcf1 with the promoter of Tmem27. A 150 bp region spanning binding sites 1 and 2 was amplified with PCR. This interaction

could not be found in primary hepatocytes, which do not express Tmem27. ChIP for Tcf1 was validated in primary hepatocytes by amplification of a region in apolipoprotein M (apoM) promoter that spans the Tcf1 binding site (Richter et al., 2003).

2.2. Pdx-1 binds to a conserved site in Tmem27 promoter

The promoter analysis of Tmem27 also revealed a conserved binding site for the β cell specific transcription factor Pdx-1. This binding site is embedded in a Tcf1 binding site, termed “site 2” in figure 5. Co-expression of Pdx-1 with Tmem27 promoter cloned upstream of the luciferase reporter gene led to a significant increase in luciferase activity compared to co-transfection with empty expression vector (Figure 9). EMSA in MIN6 cell extracts showed that ³²P-labelled probe for site 2, but not site 1, formed DNA/Pdx1 complexes upon addition of the extracts and this interaction can be further shifted with the addition of an anti-Pdx-1 antibody (Figure 7).

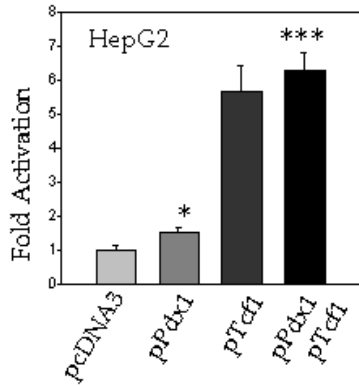


Figure 9. Transcriptional activation assay in HepG2 cells that were transfected with pcDNA3, pPdx1 or pTcf1, pCMV- β -galactosidase, and pT27luc-wt. *: $P < 0.05$, ***: $P < 0.001$.

2.3. TMEM27 is regulated during pancreas development

Expression of *Tmem27* was studied during mouse pancreatic development by immunohistochemical staining. In newborn and adult pancreas, *Tmem27* expression is restricted to β cells of the islet (Figure 3A). During development of the pancreas, *Tmem27* is expressed at the earliest time when hormone positive (mainly glucagon-positive cells) are apparent. At embryonic days E10.5 and E12.5 *Tmem27* expression is localized in cells that express glucagon and insulin. During the period of endocrine cell expansion, from embryonic day 13.5 to 18.5, *Tmem27* mainly co-localizes with glucagon until right before birth at E18.5 when it is also detected in insulin positive cells (Figure 10). *Tmem27* expression throughout development is specifically localized to hormone-positive cells. At E15.5 in the mouse, *Ngn3* expression peaks and marks the endocrine precursor cells. These cells do not express any of the endocrine hormones and subsequently, *Tmem27* expression does not co-localize with *Ngn3* (Figure 10).

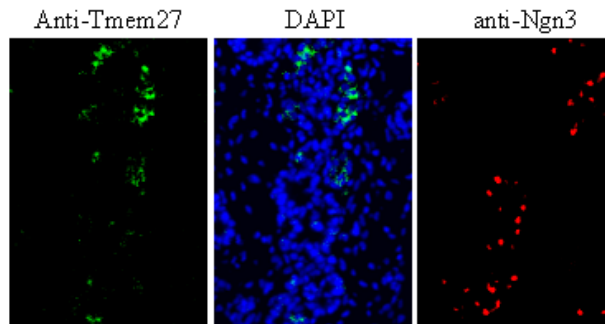
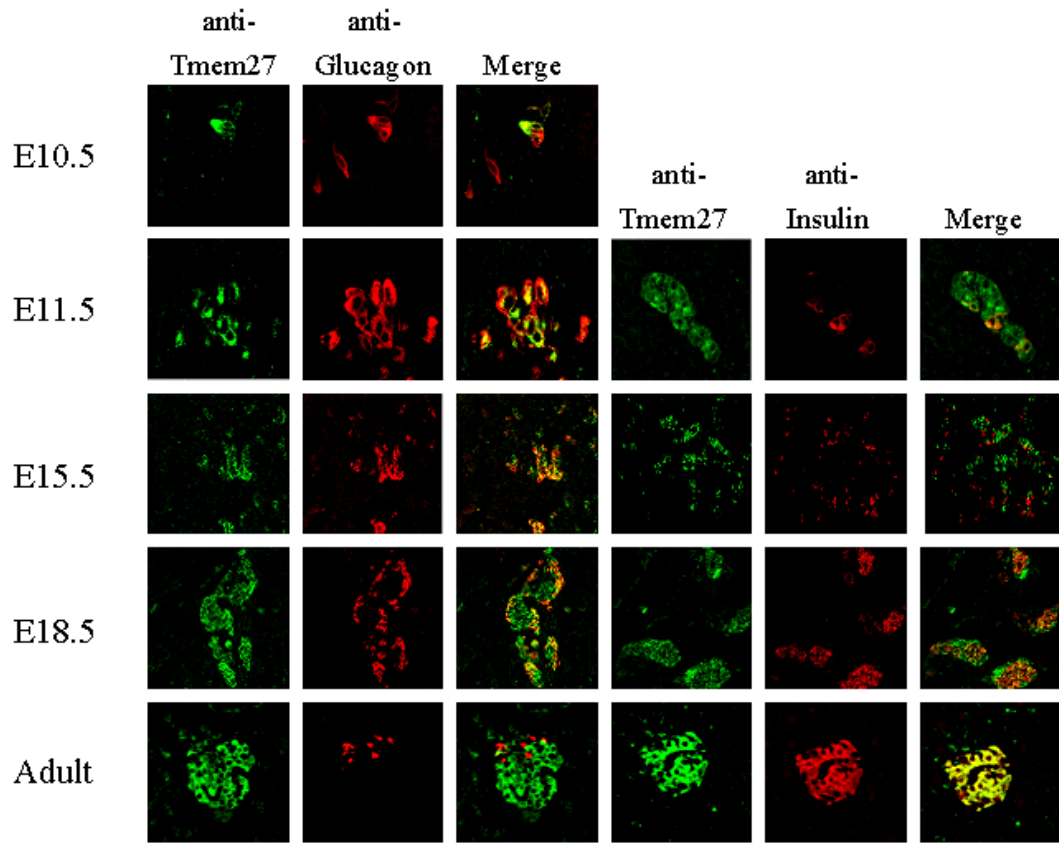


Figure 10. Tmem27 is expressed in the developing mouse pancreas

Immunofluorescence of paraffin embedded pancreatic tissue from denoted time points in the mouse development with α -Tmem27C, α -Insulin and α -Glucagon antibodies. Developmental stages are indicated as embryonic (E) days.

Immunofluorescence with α -Tmem27C and α -Ngn3 in consecutive sections of E15.5 pancreas.

2.4. Tmem27 is an N-linked glycoprotein and forms dimers *in vivo*

Tmem27 contains two predicted N-glycosylation sites at amino acid residues 76 and 93, respectively. MIN6 cells were treated with tunicamycin, an inhibitor of N-glycosylation (Waechter and Lennarz, 1976). Cells were incubated in the presence of increasing concentrations of tunicamycin and protein extracts were prepared and analyzed by SDS-PAGE and immunoblotting. Two bands with increased electrophoretic mobility appeared upon treatment with tunicamycin, whereas the high molecular weight protein disappeared (Figure 11). This result was confirmed with an *in vitro* assay using N-glycanase, an enzyme that releases intact N-linked glycans (Figure 11). These data suggest that Tmem27 is an N-linked glycoprotein.

I also carried out chemical cross-linking experiments to test if Tmem27 protein exists as a multimer. MIN6 cell extracts were incubated in the presence of two different cross-linking reagents: BMH (bismaleimido-hexane), a membrane-permeable, non-cleavable compound and DTBP (dimethyl 3, 3'-dithiobispropionimidate), a membrane permeable, cleavable compound. Following these treatments, an SDS-PAGE analysis was performed under reducing and non-reducing conditions (Partis et al., 1983; Geisler et al. 1992). Non-reducing western blots revealed a band of exactly twice the molecular weight than under reducing conditions. Cell extracts treated with BMH showed

the dimer protein in both reducing and non-reducing blots. In contrast, the protein dimers disappeared under reducing conditions in the presence of DTBP (Figure 12). The results were similar in MIN6 cells that endogenously express Tmem27 and in N2A cells that were transiently transfected with Tmem27 expression vector (Figure 12).

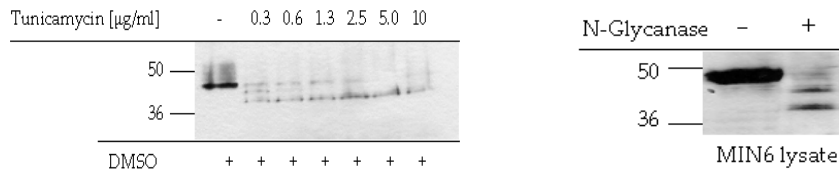


Figure 11. MIN6 cells were incubated with increasing amounts of tunicamycin, which inhibits glycosylation at asparagine residues. Addition of DMSO alone to the cells had no effect.

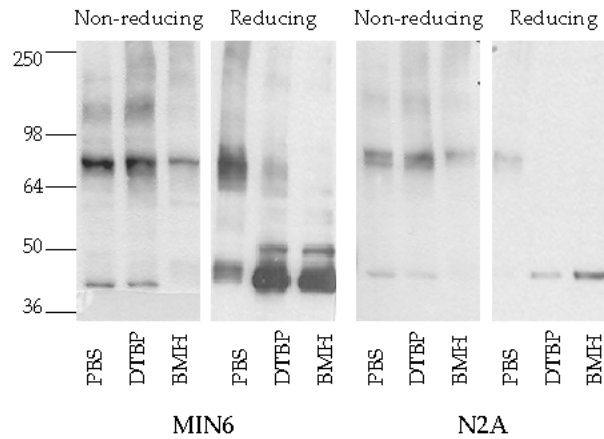


Figure 12. MIN6 cell lysates were incubated with either PBS, or cross-linking reagents dimethyl 3, 3'-dithiobispropionimidate (DTBP) and bismaleimido-hexane (BMH). SDS-PAGE under non-reducing conditions and immunoblotting using anti-Tmem27C antibodies showed a band twice the molecular weight of full-length Tmem27. Under reducing conditions, only the monomer was detected in PBS and DTBP-treated cell lysates. In contrast, the dimer persisted in BMH-treated samples as BMH cross-linking could not be reversed.

2.5. Tmem27 is cleaved and shed from pancreatic β cells

Tmem27 has previously been predicted to be a transmembrane protein with an N-terminal extracellular domain (Zhang et al., 2001). We generated two antibodies (α -Tmem27N and α -Tmem27C) that recognize peptides from extra- and intracellular domains of the protein, respectively (Figure 13). In Western blotting experiments α -Tmem27C detected two bands in whole cell lysates of MIN6 cells (Figure 14). The higher molecular weight band corresponded to the predicted molecular weight of the glycosylated full-length protein. The lower band (\approx 25 kD) was also specific since it could be detected by Western blotting in cell lysates following transfection with a vector (p-Tmem27.V5) expressing a C-terminal V5-Tag fusion protein and an anti-V5 antibody (Figure 14).

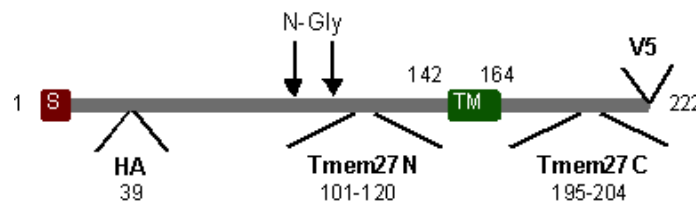


Figure 13. Schematic drawing of TMEM protein domains, including regions against which anti-peptide antibodies were raised and epitopes were inserted. Numbers denote positions of amino acid residues. S: Signal peptide sequence; TM: transmembrane domain; N-Gly: N-glycosylation sites; HA: position of HA-epitope insertion; V5: position of V5-epitope insertion; Tmem27N and Tmem27C indicate positions of sequences used for anti-peptide antibody production.

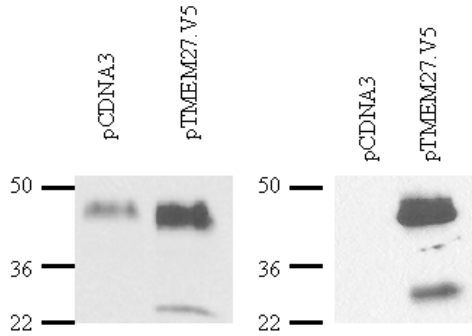


Figure 14. Anti-Tmem27C antibody in Western blots of MIN6 cells detected two bands for Tmem27 (left panel). The 25 kDa band became more abundant in cells that were transfected with pTmem27.V5. Immunoblots of cell lysates from above were probed with α -V5 antibody (right panel). The antibody against the V5-epitope also detected both bands in pTmem27.V5 transfected cells but not in pcDNA3 transfected cells.

I hypothesized that Tmem27 might be cleaved and possibly shed, with the lower molecular weight band representing the C-terminal transmembrane spanning part of Tmem27. I therefore analyzed supernatants from different cell lines (including neuronal N2A cells, HepG2 cells, HEK293 and M-1 cells that were derived from collecting ducts of the kidney and which exhibit endogenous expression of Tmem27). Cells were cultured for 48 h in reduced serum medium and Tmem27 immunoreactivity in the supernatant was assayed by Western blotting using α -Tmem27N. I detected a band corresponding to a \approx 25kDa protein in clonal β cell lines MIN6 and INS1E (Figure 15). Interestingly, this protein can only be detected in the supernatant but not in whole-cell lysates, indicating that cleavage occurs at the outer plasma membrane. This cleaved form of Tmem27 could also be detected in media incubated with isolated mouse pancreatic islets

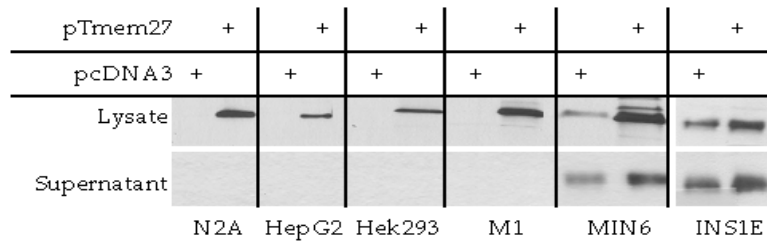


Figure 15. Denoted cell lines were transfected with pcDNA3 or pTmem27 and full length protein was detected with anti-Tmem27C in Western blots of cell lysates. Secreted protein was detected with anti-Tmem27N only in the supernatant of MIN6 cells. Increased expression of full-length protein led to increased amounts of secreted protein solely in the β cell lines (MIN6 and INS1E). Supernatants were normalized to protein content of cell lysates.

(Figure 16). Treatment of supernatants with N-Glycanase led to the disappearance of the ≈ 25 kDa protein and the emergence of a band at ≈ 12 kDa, the expected molecular weight of the unglycosylated N-terminal domain of Tmem27 (Figure 17). Interestingly, in spite of robust expression of full-length protein in cell-lysates, I failed to detect this band in Western blot analysis in the culture medium of non- β cell lines that were transiently transfected with a Tmem27

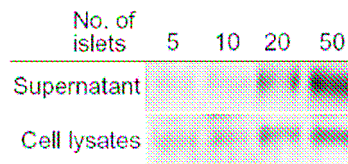


Figure 16. Mouse pancreatic islets were isolated and incubated for 72 hrs. Supernatants were collected and islets were transferred in lysis buffer. Full-length protein was detected with anti-Tmem27C in Western blots of lysates and secreted protein was detected with anti- anti-Tmem27N in Western blots loaded with equal volumes of the supernatant.

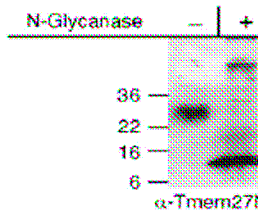


Figure 17. Supernatant from MIN6 cells was incubated with N-glycanase. The molecular weight shift in the Western blot indicates that the enzyme removed sugar moieties from secreted Tmem27. Secreted protein was detected with anti-Tmem27N antibody.

expression vector (pTmem27). In contrast, over-expression of Tmem27 in MIN6 and INS1E cells led to increased amounts of secreted protein in their culture media (Figure 15). I also showed that siRNA-mediated reduction in Tmem27 protein levels correlated with decreased levels of the secreted form of Tmem27 in MIN6 cell supernatants (Figure 18).

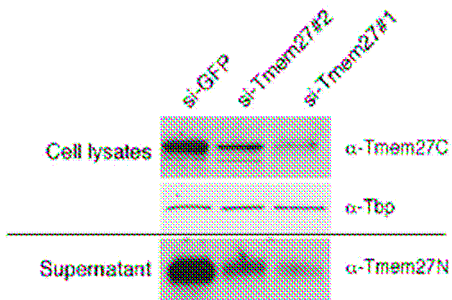


Figure 18. MIN6 cells were electroporated with siRNAs targeting GFP or Tmem27. In the cells that were electroporated with si-Tmem27#1 and #2, reduction in the levels of Tmem27 protein was detected with anti-Tmem27C 48 hrs after electroporation. SDS-PAGE was run with Supernatants from the same cells and reductions in the levels of secreted proteins were detected with anti-Tmem27N. Supernatants were normalized to protein content of cell lysates.

Lastly, in order to irrefutably prove that N-terminal portion of Tmem27 is cleaved and secreted from β cells an expression vector (pTmem27-HA) was generated in which a nine amino acid HA-epitope tag was inserted downstream

of acid residues 39 of the Tmem27 protein (Figure 13). MIN6 cells transfected with this vector secreted a protein in the supernatants that could be detected with an anti-HA antibody and had a similar size as untagged Tmem27. This protein was not detected in control cells or cells expressing the untagged protein (Figure 19). Together, these data demonstrate that Tmem27 is a pancreatic β cell-specific, cleaved and shed transmembrane protein.

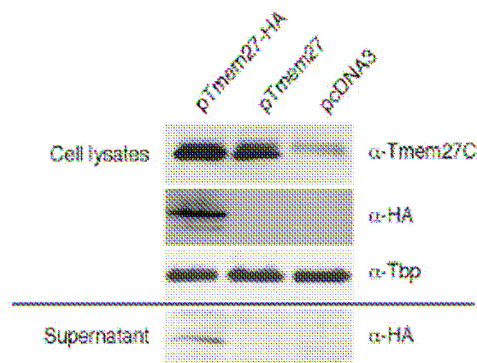


Figure 19. MIN6 cells were electroporated with pcDNA3, pTmem27 or pTmem27-HA. Overexpression of Tmem27 was detected by Western blotting of cell lysates with anti-Tmem27C antibodies. Supernatants from the same cells were subjected to Western blotting with anti-HA epitope antibody.

2.6. Tmem27 is a constitutively shed plasma membrane protein

To localize Tmem27 in pancreatic β cells, I performed immunofluorescence studies using anti-Tmem27N and -C antibodies. MIN6 or dispersed pancreatic islets were grown on slides, fixed and permeabilized and treated with primary antibodies raised against insulin and synaptophysin (*Syn*), specific markers for insulin-containing dense-core granules and synaptic-like microvesicles, respectively (Wiedenmann et al., 1988). Neither insulin nor synaptophysin co-localized with Tmem27, demonstrating that Tmem27 is not a constituent of these organelles (Figure 20).

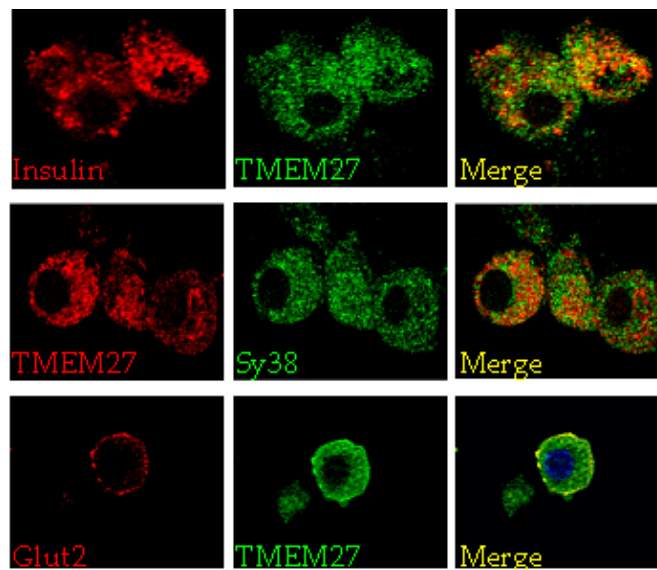


Figure 20. Isolated mouse islets were dispersed and stained with anti-Tmem27C and anti-Insulin, anti-Synaptophysin or anti-Glut-2 antibodies.

Subcellular fractionation of MIN6 cells with a sucrose density gradient also showed that Tmem27 was not in the same vesicles as insulin or prohormone convertase 1/3 (PC1/3), a protease that cleaves insulin and resides in the dense core vesicles with insulin. Tmem27 appears to localize to similar-sized vesicles as synaptic-like microvesicles as immunoreactivity was detected in the same samples with Syn (Figure 21).

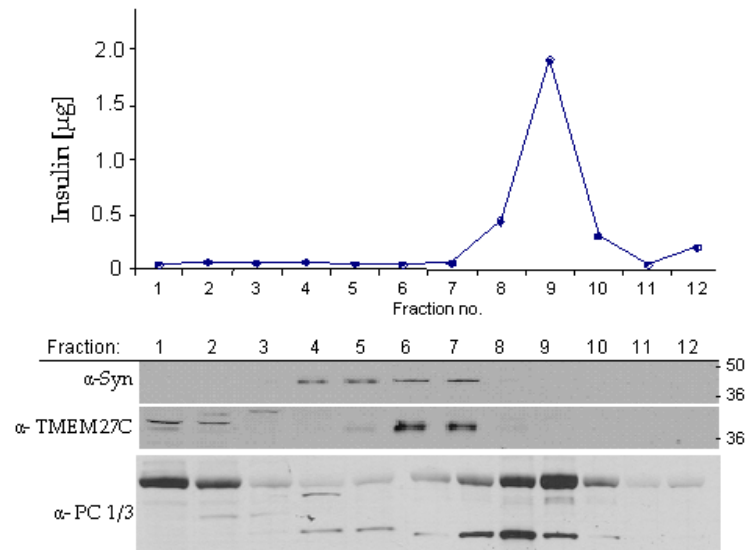


Figure 21. MIN6 cells were fractionated in a linear sucrose density gradient. Insulin levels were measured using a radioimmunoassay (RIA) for rat insulin. All fractions were subjected to SDS-PAGE and immunoblotted with α -Syn, α -Tmem27C, and α -PC1/3.

Specific staining of Tmem27 was detected in the perinuclear compartment and on the plasma membrane. Plasma membrane staining of Tmem27 co-localized with membrane immunoreactivity of Glut2, further supporting that Tmem27 is a surface-membrane protein (Figure 20). We also studied Tmem27 by electron

microscopy and observed nanogold particles associated with the plasma membrane in proximity to vesicle /membrane fusion events (Figure 22).

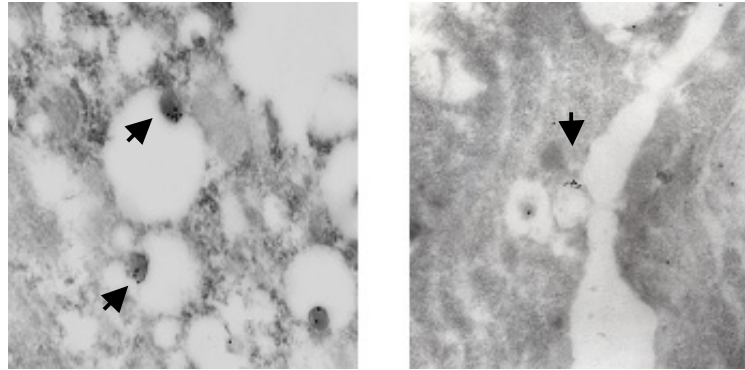


Figure 22. Electron microscopy performed on MIN6 cells with anti-Tmem27C antibodies localized Tmem27 in small secretory vesicles (arrows). IgG conjugated to 10 nm gold particles was used for detection of the antibody. (Right Panel) vesicles that contain Tmem27 were detected during fusion events with the plasma membrane (arrow).

To further investigate the release of the cleaved form of Tmem27 I stimulated isolated pancreatic islets cells with low (2.8 mM) and high (11.1 mM) glucose concentrations. Whereas insulin secretion increased when stimulated with glucose I did not measure a change in Tmem27 concentrations in the supernatant of these cells (Figure 23). I repeated the experiment in MIN6 cells by incubating the cells in media with low (5.5 mM) and high (25 mM) levels of glucose and observed that Tmem27 shedding did not follow insulin secretion dynamics (Figure 24).

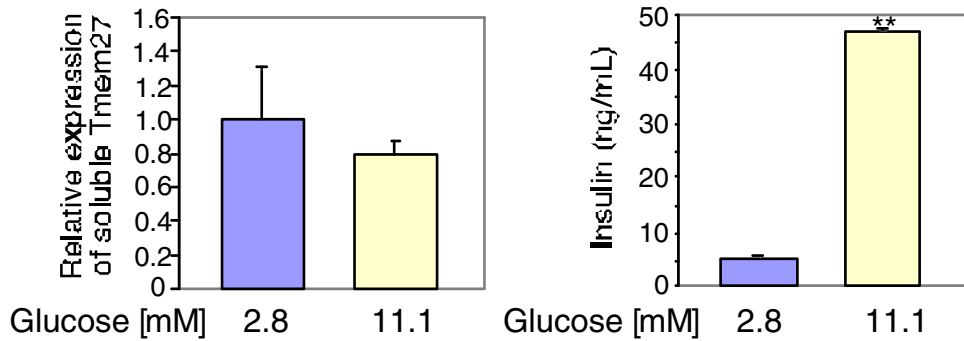


Figure 23. An equal number of size-matched mouse islets were incubated in either 2.8 mM or 11.1 mM glucose. Supernatants were collected after 72 h and soluble Tmem27 levels were quantified and normalized to protein content of islet lysates. Secreted insulin levels were measured after 6 h incubation in the same supernatant. **: P<0.0002.

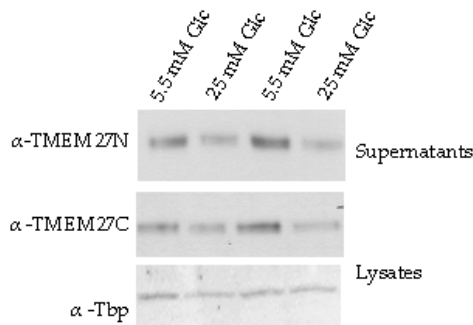


Figure 24. MIN6 cells are incubated in 5.5 mM or 25 mM glucose. Supernatants were collected after 6 hrs and immunoblotted with α-Tmem27N. Cell lysates were also collected to detect full-length protein with α-Tmem27C. Protein content of wells were assessed with α-Tbp antibody.

Lastly, I performed pulse-chase experiments using ³⁵S-methionine to determine the kinetics of uncleaved and soluble Tmem27 proteins. [³⁵S]methionine incorporation in Tmem27 was calculated from band densities on scanned autoradiography films. Relative immunoprecipitated radioactivity on the gels showed that [³⁵S]methionine was incorporated in Tmem27 protein for up to 3 hours after the start of the chase period. This timepoint is denoted as 100%

incorporation (Figure 25). The half-life of Tmem27 from linear regression analysis of the data points was determined to be ≈ 27 hours. [^{35}S]-labeled soluble Tmem27 was immunoprecipitated from MIN6 supernatants and quantitated by scintillation counting after PAGE. Relative radioactivity present in the bands over a period of 24 hours revealed that the amount of cleaved Tmem27 in the supernatant of MIN6 cells increased linearly and by approximately 10% every hour. These data show that soluble Tmem27 is shed into the supernatant in a constitutive manner.

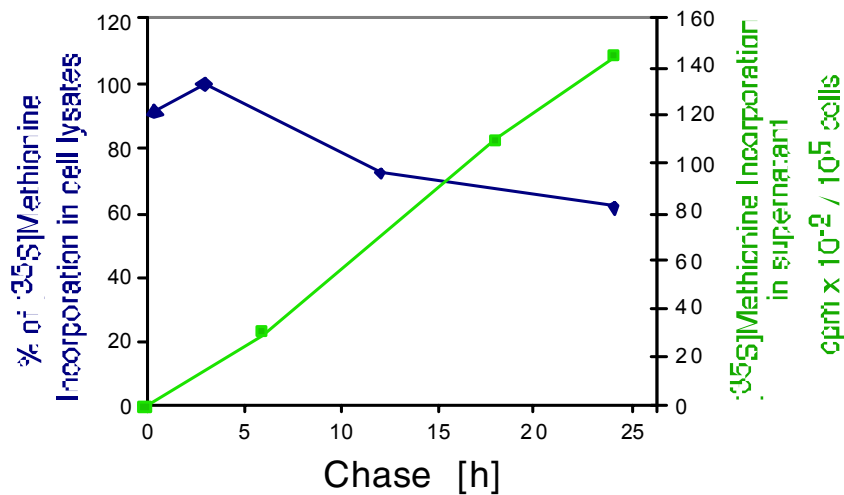


Figure 25. [^{35}S]Methionine incorporation into Tmem27 was measured in MIN6 cells during a pulse-chase experiment over 24 hrs.

2.7. Search for a cleavage site and protease

In order to further characterize the shedding of soluble Tmem27, I attempted to determine the exact site of cleavage by mass spectrometry. I ran immunoprecipitated protein from MIN6 supernatants on SDS-PAGE (Figure 26) and excised the band for amino acid sequence determination. This method was unsuccessful most likely because glycosylation on the protein hinders the process.

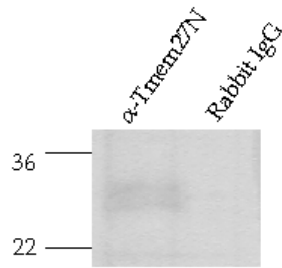


Figure 26. Immunoprecipitated Tmem27 from supernatants of MIN6 cells was detected with Coomassie blue. Rabbit IgG was used as a control.

Interestingly ectodomain shedding of Tmem27 is a very β cell specific event. Initially this observation led to the hypothesis that the protease responsible for the generation of soluble Tmem27 is a β cell-specific or -enriched enzyme. Analysis of the amino acid sequence revealed a putative conserved proprotein convertase cleavage site at residues 106-111 (RXXR/KXR) (Figure 27). The major endoproteolytic processing enzymes of endocrine cell secretory pathway are the subtilisin-like proprotein convertases. In the β cell, members of this family such as furin, prohormone convertase 1/3 (PC1/3) and prohormone

convertase 2 (PC2) function in cleavage of insulin and other peptides (Steiner, 1998). Functionality of the cleavage site was investigated by PCR site-directed mutagenesis. Depending on the particular site arginines and/or lysines are the key residues in proprotein convertase cleavage. Therefore, I generated two mutated versions of pTmem27.V5. Arginine at 106 and lysine at 109 were mutated to isoleucine and alanine, respectively in one expression vector (pT27-R106K109) and the arginine at position 111 was changed to a leucine in a second expression vector (pT27-R111). The mutated versions of Tmem27 migrated differently compared to wild-type Tmem27 on SDS-PAGE (Figure 27). However, the protein was cleaved successfully as increased soluble form was detected in the supernatants of all MIN6 cells and on western blots using α -Tmem27N, the lysates showed both the full-length form and the C-terminal fragment left upon cleavage (Figure 27). In order to exclude the involvement of the known β cell proprotein convertases as well as that of carboxypeptidase E (exopeptidase necessary for efficient endoproteolytic processing of proinsulin and several other protein precursors) in Tmem27 shedding, siRNAs were used to reduce the expression of these proteases in MIN6 cells. Reduced expression of furin, PC1/3, PC2 or carboxypeptidase E in MIN6 cells did not have an effect on the levels of soluble Tmem27 in the supernatant of these cells (data not shown). These findings were also supported by data in results section 2.6 where Tmem27 was

localized to vesicles separate from insulin containing secretory granules where the prohormone convertases reside.

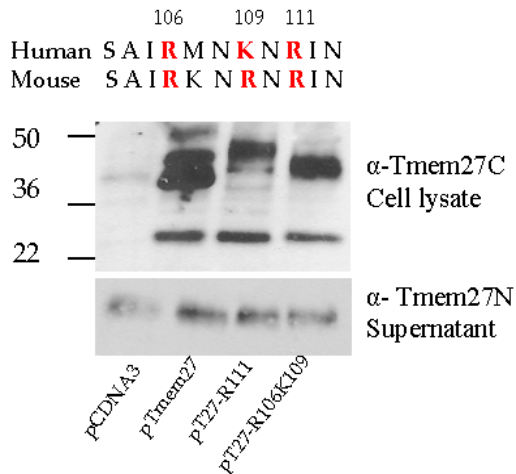


Figure 27. There is a putative prohormone convertase site in both human and mouse Tmem27 sequence. The important residues for cleavage are highlighted in red. The denoted sequences are mutated on pTmem27 expression vector.

Various non-β cell lines were tested for Tmem27 shedding with negative results. Examination of the data from Affymetrix™ array of Tcf1^{-/-} islets revealed regulation of hepatocyte growth factor activator (HGFA) expression. Expression levels of HGFA was markedly reduced in the islets of Tcf1^{-/-} mice compared to wild-type controls. Two experiments were performed to investigate the possibility of a role HGFA might play in Tmem27 cleavage. First, isolated primary hepatocytes were infected with an adenovirus expressing the human Tmem27 protein (Adv-hTmem27). Supernatants were run on SDS-PAGE and blotted with α-Tmem27N to detect soluble protein. Figure 28 shows that even though a high level of Tmem27 expression was achieved in isolated hepatocytes,

no protein shedding occurred in the supernatants 48hrs after infection. Secondly, neither over-expression of HGFA protein nor reduction of its expression with several siRNAs had any effect on the levels of soluble Tmem27 in the supernatants of MIN6 cells (data not shown).

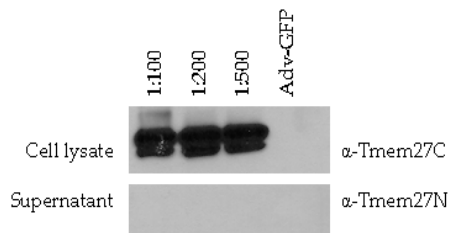


Figure 28. Isolated primary hepatocytes are infected with either increasing amounts of Adv-hTmem27 or Adv-GFP at 1:200 dilution. Cells were incubated in OPTI-MEM for 48 hrs and subjected to SDS-PAGE along with cell lysates.

The possibility of the protease that cleaves Tmem27 being a soluble enzyme in MIN6 supernatant was explored by co-culture studies of MIN6 and COS7 cells. COS7 cells were transfected with either pcDNA3 or pTmem27-HA and seeded in 6 well plates. MIN6 cells were plated in cell culture inserts on top of the COS7 cells and incubation was continued for 48 hours. Supernatants were immunoblotted with α -HA antibody and α -Tmem27N to detect the released protein from either cell type. Figure 29 shows that soluble protein from MIN6 cells could be detected in COS7 supernatant demonstrating that co-culture system was functional, however, no HA tagged protein could be detected as MIN6 supernatant was not able to induce release of Tmem27 from COS7 cells.

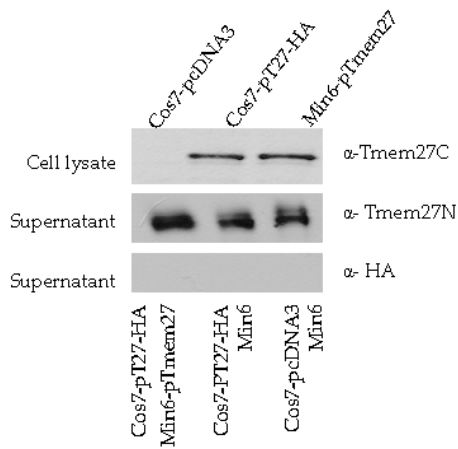


Figure 29. COS7 cells were transfected with either pcDNA3 or pTmem27-HA and co-cultured with MIN6 cells that were electroporated with pcDNA3 or pTmem27.V5. Top legend shows overexpression of Tmem27 in COS7 and MIN6 cells. Bottom legend denotes two layers of the co-culture setup.

Ectodomain shedding is an important regulatory mechanism in the function of membrane-bound cell-surface molecules (Arribas and Borroto, 2002) and the most widely studied inducer of shedding is phorbol 12-myristate 13-acetate (PMA), which activates protein kinase C (Schlondorff and Blobel, 1999). Upon incubation of MIN6 cells with PMA, shedding of Tmem27 was also stimulated. MIN6 cells were incubated in either 1 μ M PMA or DMSO in OPTI-MEM for 1.5 hours and Figure 30 shows that cells, that were stimulated with PMA, had significantly more soluble Tmem27 in the media. Upon this finding, I investigated whether other cell types that do not endogenously express Tmem27 would be able to shed the ectodomain with PMA stimulation. COS7 cells were transfected with pTmem27.V5 and 48 hours later they were stimulated with PMA for 6 hours. The supernatant from PMA and DMSO treated cells were immunoblotted with α -Tmem27N. PMA stimulated COS7-pTmem27.V5 showed

no bands at 25 kDa where soluble Tmem27 migrates compared to DMSO treated COS7-pTmem27.V5 (Figure 30).

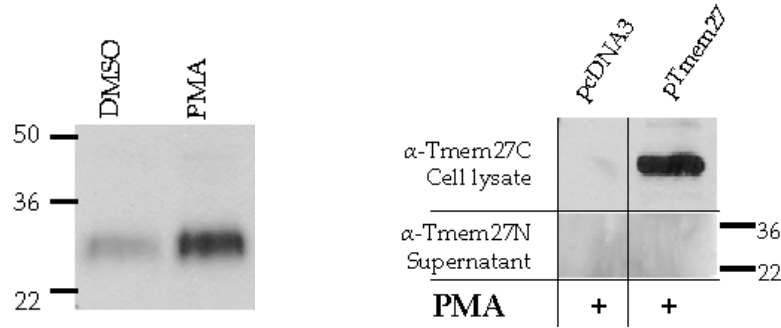


Figure 30. Stimulation of ectodomain shedding in MIN6 and COS7 cells with PMA.

Next a selective screening approach was taken to possibly identify the type of protease involved in the release of soluble Tmem27. MIN6 cells were incubated in OPTI-MEM with various protease inhibitors at different concentrations for 3hr, 6hr, and 12hr periods. Table 2 displays the different protease inhibitors used as well as their specificity for protease inhibition. As seen in Figure 31 and 32, none of the protease inhibitors had an effect on the shedding of Tmem27 in MIN6 cells except for BB94, which is a metalloprotease inhibitor.

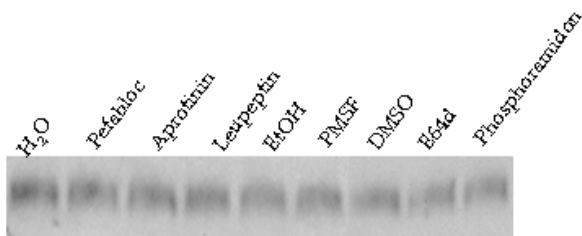


Figure 31. MIN6 cells were incubated in OPTI-MEM supplemented with denoted protease inhibitors for 3hours and supernatants were immunoblotted with α-Tmem27N.

Table 2. Protease inhibitors that were used on MIN6 cells

Inhibitor	Substrates	Working Concentration
Pefabloc	Broad serine protease inhibitor	0.1 mg/ml
Aprotinin	Serine protease inhibitor	0.01-3 μ g/ml
Leupeptin	Serine and cysteine protease inhibitor	10-100 μ M
PMSF	Serine and cysteine protease inhibitor	0.1-1 μ M
E64d	Cysteine protease inhibitor	10 μ M
Phosphoramidon	Inhibitor of metalloendopeptidases	100 μ M
BB94	Metalloprotease inhibitor	1 μ M

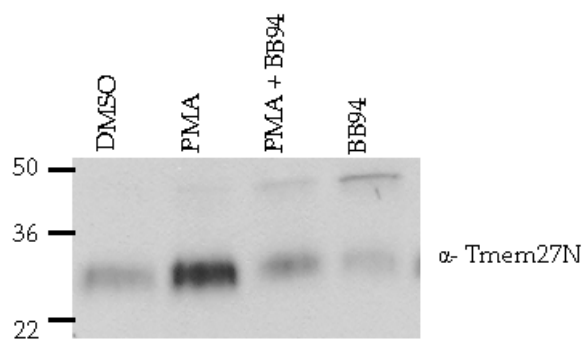


Figure 32. MIN6 cells were incubated in OPTI-MEM supplemented with DMSO or 1 μ M PMA for 1.5 hrs for stimulation of ectodomain shedding. For inhibitor experiment, MIN6 cells were either incubated with 1 μ M BB94 alone or 1 μ M PMA and 1 μ M BB94 for 1.5 hrs.

Remarkably, BB94 was also able to inhibit stimulation of Tmem27 shedding by PMA (Figure 32). BB94 (batimastat) is a hydroxamate-based competitive inhibitor and has been shown to inhibit activity of many metalloprotease disintegrins (ADAM family of proteases) and certain ADAMs have been shown to be mediators of PMA stimulated ectodomain shedding (Black et al., 1997). Three members of this family, ADAM9, ADAM10 and

ADAM17, have been studied in the mouse pancreas and display specific developmental and adult expression patterns (Asayesh et al., 2005). ADAM9 expression gets restricted to β cells in adult mouse pancreas. Two approaches were taken to see whether ADAM9 is involved in Tmem27 cleavage. SiRNA targeted reduction in ADAM9 expression in MIN6 cells had no effect on soluble Tmem27 generation (data not shown). Moreover, islets isolated from ADAM 9^{-/-} 15^{-/-}12^{-/-} triple knockout (Sahin et al., 2004) mice release similar amounts of Tmem27 in their supernatants as islets isolated from wild-type control mice (Figure 33).

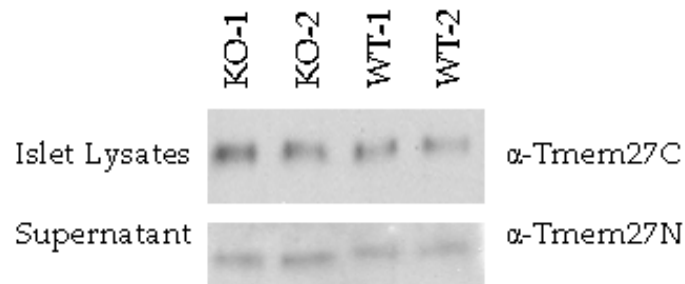


Figure 33. Isolated islets from ADAM 9^{-/-}15^{-/-}12^{-/-} and control animals were incubated for 48 hrs in OPTI-MEM and immunoblotted with α -Tmem27N.

2.8. Tmem27 influences insulin secretion

Glucose stimulated insulin secretion was measured in MIN6 cells with increased and reduced Tmem27 expression. MIN6 cells were transfected with either pcDNA3 or pTmem27.V5. MIN6 cells were stimulated with glucose or KCl 48 hours post transfection and insulin released into the media was measured. Increased expression of Tmem27 significantly reduced insulin release from MIN6 cells (Figure 34). In parallel, reducing expression of Tmem27 with siRNAs led to a significant increase in glucose stimulated insulin secretion (Figure 35). Increased and reduced expression of Tmem27 had no effect on the insulin content of MIN6 cells (Figure 36).

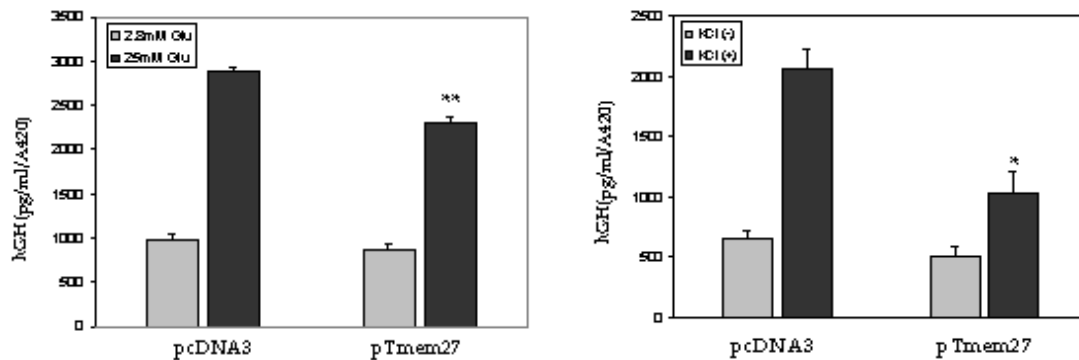


Figure 34. Glucose- (2.8 mM or 25 mM) and KCl (60mM)-stimulated insulin secretion in MIN6 cells 48 hours after they were transfected with pcDNA3 or pTmem27.V5. *: $P < 0.05$, **: $P < 0.01$.

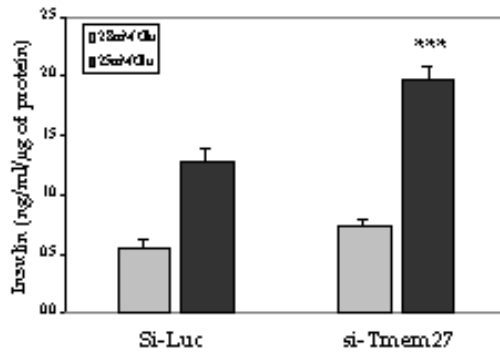


Figure 35. Glucose-stimulated insulin secretion in MIN6 cells that were transfected with a siRNA against luciferase (si-Luc) or si-Tmem27. ***: $P < 0.001$.

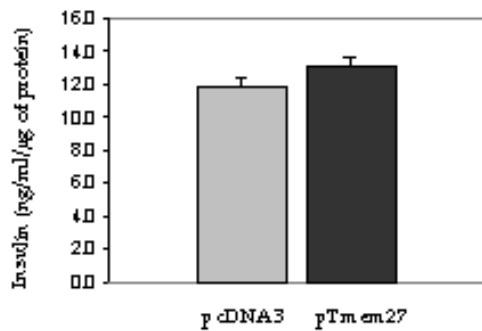


Figure 36. Insulin content of MIN6 cells was measured by acid/ethanol extraction and normalized per protein content of each sample. There was no significant difference in insulin content of MIN6 cells transfected with pcDNA3 or pTmem27.

A recent paper also described a role for Tmem27 in insulin secretion (Fukui et al., 2005). The authors proposed that full-length Tmem27 augments insulin secretion in INS1 cells. They postulated a function for Tmem27 in insulin exocytosis through its interaction with a SNARE complex component called snapin. Fukui et al. further showed immunoprecipitation data that associated Tmem27 with other SNARE complex proteins such as SNAP25 and VAMP2. Since the aforementioned data contradicted my findings in Figure 34 and 35, I attempted to reproduce some of the experiments. Tmem27 was immunoprecipitated with α -Tmem27C from MIN6 cell lysates. The eluate as

well as flow-through and the wash fractions of the experiment were subjected to SDS-PAGE and detected with α -Tmem27C. Rabbit IgG was used as a control since Tmem27 antibody was raised in rabbits. The western blot in Figure 37 showed that Tmem27 was successfully immunoprecipitated with α -Tmem27C and could also be detected in the flow-through fraction of the rabbit IgG experiment. The western blots for the same fractions using α -snapin and α -VAMP2 antibodies showed that these proteins did not precipitate with Tmem27 in MIN6 cells (Figure 37). Furthermore, Tmem27 did not co-localize with either VAMP2 or syntaxin by immunofluorescence on isolated and dispersed pancreatic islets (Figure 38).

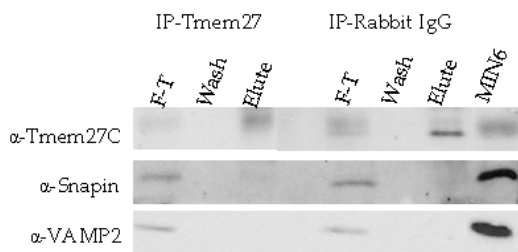


Figure 37. Immunoprecipitation of Tmem27 in MIN6 cells with α -Tmem27C. F-T: Flow-through.

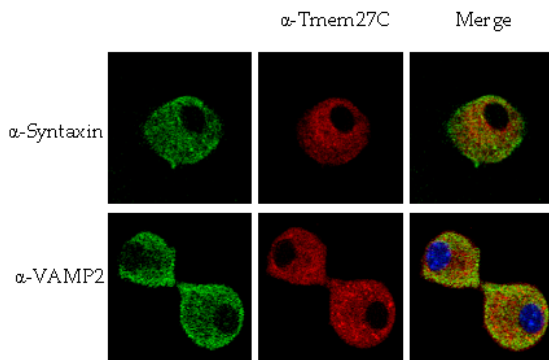


Figure 38. Immunofluorescence on isolated primary islets with α -Tmem27C, α -Syntaxin and α -VAMP2. No-colocalization of Tmem27 was detected with SNARE complex proteins.

2.9. Increased expression of TMEM27 in mouse models with islet hypertrophy and enhanced β cell replication *in vitro*

I measured expression of *Tmem27* in hypertrophied islets of *ob/ob*, *db/db* and *aP2-Srebp-1c* transgenic mice (Shimomura et al., 1998). Pancreatic islets from 6-8 week old mice were isolated and gene expression levels were compared to their wild-type littermates. Using real-time PCR I found a 1.7, 1.7 and 2.7-fold increase in *Tmem27* levels of *ob/ob*, *db/db* and *aP2-Srebp-1c* islets, respectively, compared to controls (Figure 39). In addition, islets isolated from these mice exhibited a significant increase in secretion of cleaved *Tmem27* into the medium compared to size-matched islets of wildtype littermates (Figure 40).

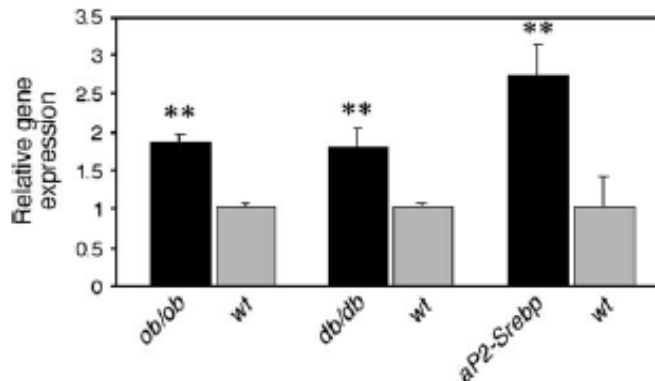


Figure 39. *Tmem27* expression levels were measured in islets isolated from *ob/ob*, *db/db*, *aP-Srebp-1c* and wildtype littermate control mice with quantitative RT-PCR. *Tmem27* expression was evaluated relative to β -actin levels in the same sample. **: $P < 0.01$

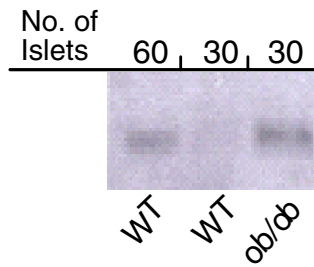


Figure 40. Isolated islets from wildtype and *ob/ob* mice were matched for number and size and incubated in equal volumes of media for 72 hrs. Secreted protein was detected with anti-Tmem27N.

Spontaneous mutant strain C57BL/KsJ *db/db* (BKS-Lepr/J) mice have the *db* mutation, a splicing mutation caused by a point mutation in the downstream intron of the leptin receptor gene, and are unresponsive to leptin. These mice have unrepressed eating behavior, become obese, and develop severe insulin resistance associated with hyperinsulinemia, hyperglycemia, and hypertriglyceridemia. These mice show increased compensatory β cell mass up to 3 months of age, however, from 3 to 6 months they drastically reduce their β cell mass resulting in severe insufficiency of insulin secretion (Kawasaki et al., 2005). I compared the expression levels of Tmem27 in islets of BKS-Lepr/J mice and their littermate controls at 3 months and 6 months of age by real-time RT-PCR. Figure 41, left panel, shows that Tmem27 expression was markedly increased at 3 months when the islets of BKS-Lepr/J mice display hypertrophy. The right panel of figure 41 shows that at 6 months old the islets of BKS-Lepr/J mice had no difference in the expression levels of Tmem27 compared to their

littermate controls. In this study, the Tmem27 expression levels were found to correlate with the islet mass of diabetic BKS-Lepr/J animals.

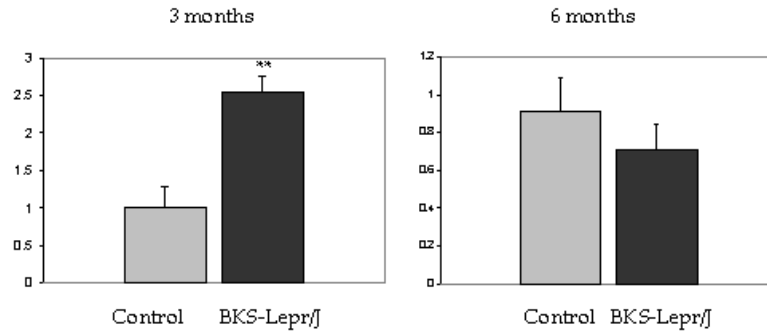


Figure 41. Tmem27 expression levels were measured in islets isolated from BKS-Lepr/J and wildtype littermate control mice with quantitative RT-PCR. Tmem27 expression was evaluated relative to β-actin levels in the same sample. **: P<0.01

To study if Tmem27 stimulates pancreatic β cell replication I examined the effect of Tmem27 expression on the proliferation of MIN6 cells. Cells were electroporated with either siRNAs targeting Tmem27 or plasmid pTmem27. Cell replication was assessed by cell counting and measuring incorporation of [³H]thymidine 48 h after electroporation (Figure 42). MIN6 cells that were transfected with pTmem27 exhibited ≈5-fold overexpression compared to pcDNA3 transfected cells and showed ≈2-fold increase in [³H]thymidine incorporation and increased cell density 48 h after plating. In contrast, MIN6 cells that had reduced expression of protein following siRNA treatment showed significantly lower [³H]thymidine incorporation and cell density (Figure 42).

Furthermore, I did not observe any changes in apoptosis in cells with increased or reduced expression of Tmem27 (Figure 43), suggesting Tmem27 it does not affect cell death.

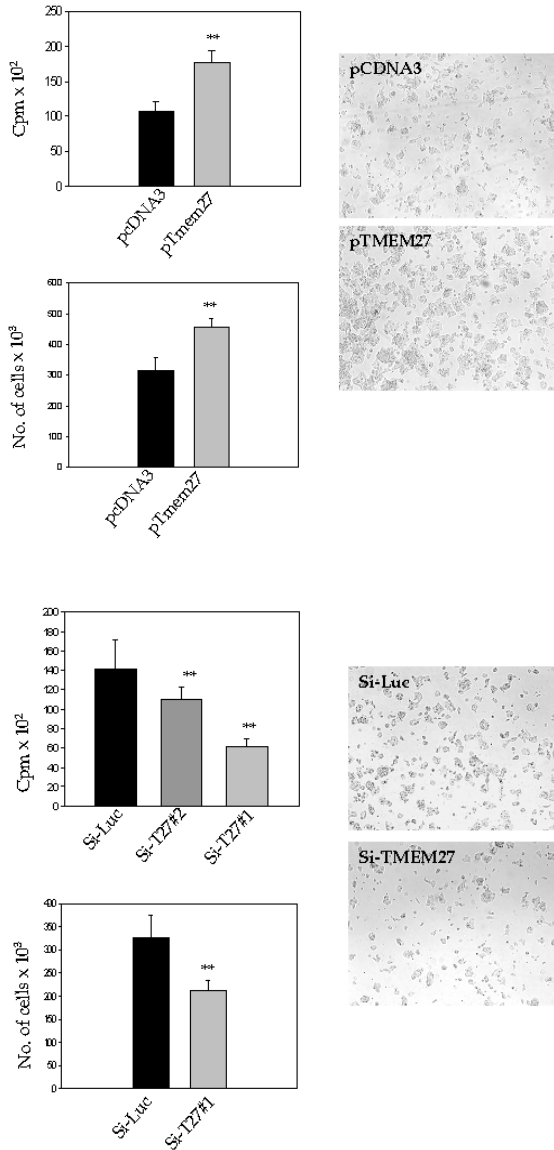


Figure 42. MIN6 cells were electroporated with siRNAs targeting luciferase or Tmem27 and pcDNA3 or pTmem27. Cells were trypsinized 48 hrs after electroporation, stained with trypan blue and counted with a hemocytometer. Each value represents a mean of six independent experiments. Cell replication was measured by [³H]thymidine incorporation. **: P<0.01.

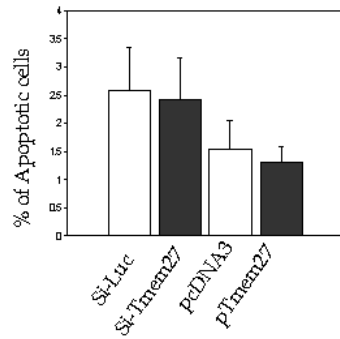


Figure 43. TUNEL assay was performed on MIN6 cells that were electroporated with siRNAs targeting luciferase or Tmem27 and pcDNA3 or pTmem27.

To further elucidate if the full-length, truncated or soluble form of Tmem27 stimulated β cell replication *in vitro* I generated a Tmem27 mutant (pTmem27-V5.del.) in which amino-acid residues 17-129 were deleted. Transfection of pTmem27-V5.del. in MIN6 cells led to the expression of a truncated protein of ≈ 30 kDa (Figure 44). [3 H]thymidine incorporation assays demonstrated that expression of the full-length Tmem27 increased replication not only in MIN6 cells but also in HepG2 and HEK293 cells. In contrast, over-expression of the truncated Tmem27 form showed no effect (Figure 45). I confirmed by immunofluorescence and cross-linking experiments that the truncated Tmem27 reached plasma membrane and was able to dimerize in MIN6 cells (Figure 46). Since non- β cell lines do not release the soluble Tmem27 form these data demonstrate that the full-length form of Tmem27 is responsible for the proliferation response. Independent evidence that the soluble form has no effect

on cell replication was obtained from co-culture and conditioned medium experiments in which cells were cultured with increasing concentrations of soluble Tmem27 (Figure 47 and 48). Together, these results demonstrate that the full-length form of Tmem27 stimulates cell proliferation in MIN6 and other cell types.

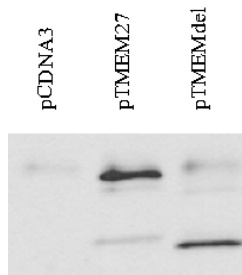


Figure 44. MIN6 cells were electroporated with pcDNA3, pTmem27-V5, or pTmem27-V5del, which lacks amino acid residues 17-129. The deletion mutant is expressed as a \approx 30kDa protein.

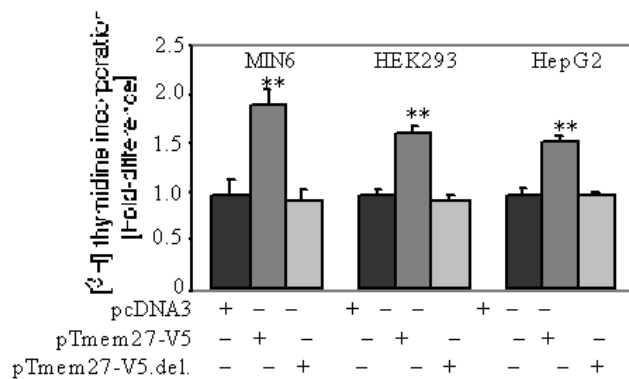


Figure 45. MIN6, HepG2 and HEH293 cells were transfected with pcDNA3, pTmem27-V5 or pTmem27-V5.del. Cell replication was measured by [³H]thymidine incorporation. **: P<0.01.

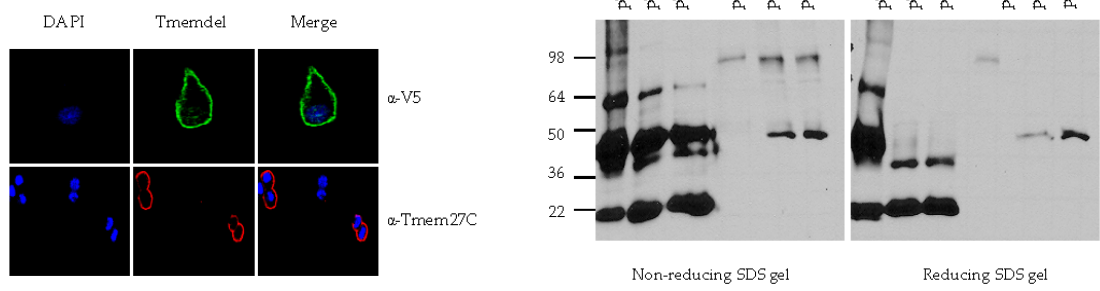


Figure 46. Immunofluorescence on MIN6 cells transfected with pTmem27-V5del showed that the deletion mutant localized to plasma membrane. Cross-linking experiment showed that the deletion mutant formed dimers in MIN6 cells.

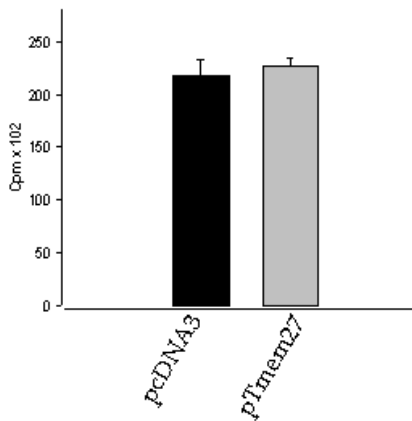


Figure 47. MIN6 cells were co-cultured with MIN6 cells electroporated with either pcDNA3 or pTmem27. Cell replication of the bottom layer was measured by ³H]thymidine incorporation.

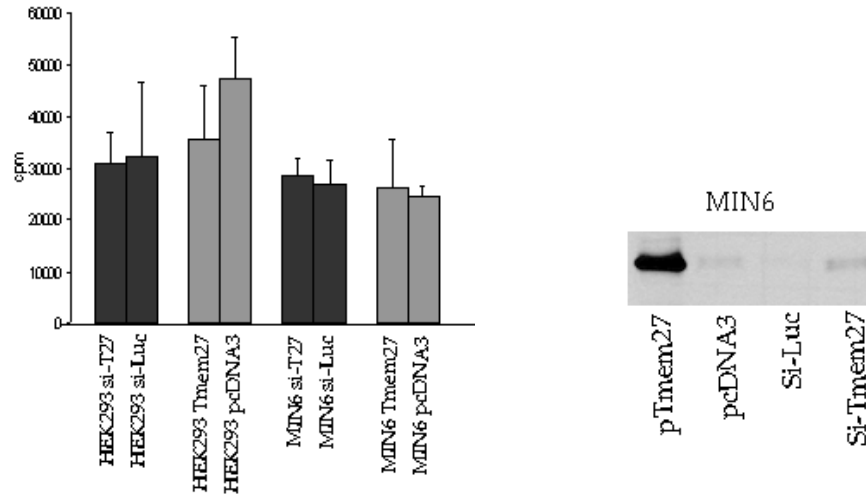


Figure 48. HEK293 and MIN6 cells were incubated with conditioned media from MIN6 cells that expressed increasing amounts of Tmem27. Cell replication of the bottom layer was measured by [³H]thymidine incorporation.

2.10. Transgenic mice overexpressing Tmem27 in pancreatic islets exhibit islet hypertrophy

We generated two independent pancreatic β cell-specific transgenic lines following pronuclear microinjection of a vector construct in which the human Tmem27 cDNA is under the control of the rat insulin promoter. RT-PCR and immunoblot analysis showed that Tmem27 expression in both lines was \approx 4-fold increased in pancreatic islets of transgenic mice compared to wildtype littermates (Figure 49).

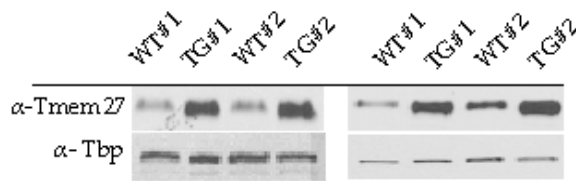


Figure 49. Increased expression of Tmem27 was detected with anti-Tmem27C in Western blots of islets isolated from both RIP-Tmem27 transgenic mice and wildtype littermate controls.

I studied the islet mass at ages 10 and 20 weeks in transgenic animals by pancreatic islet morphometry. Transgenic mice exhibited normal islet morphology (based on immunohistochemistry using insulin/glucagon co-staining) but had an approximately 1.5- and 2-fold increase in islet mass at 10 and 20 weeks respectively, compared to wildtype littermates (Figure 50 and 51). No difference was found in the mass of non- β cells (α -, δ -, and PP-cells)(Figure 52).

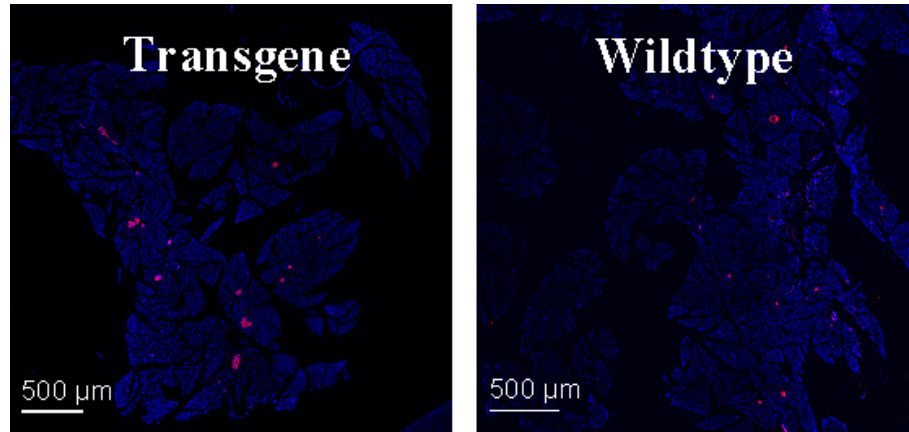


Figure 50. Immunohistochemistry of whole pancreata from transgenic and control littermate mice (n = 3). Cross-sections were embedded in paraffin and stained for insulin using anti-insulin antibodies. Images are representative of each genotype at 5x magnification.

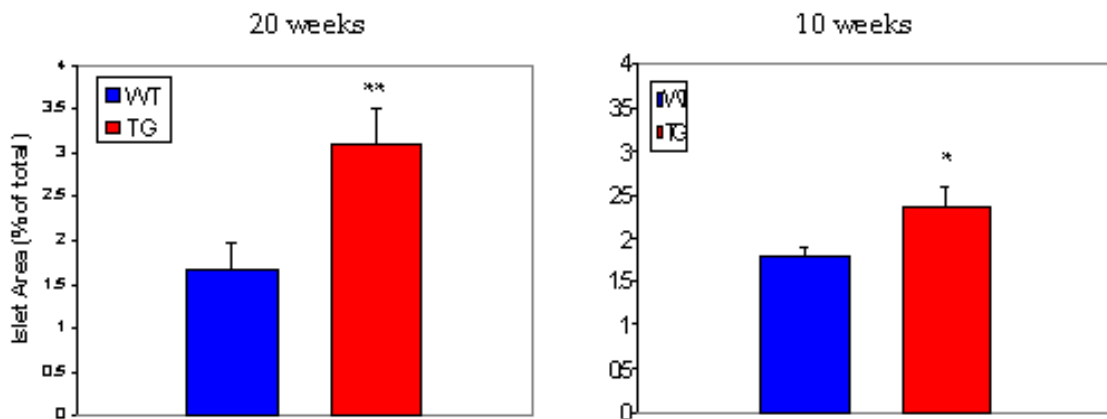


Figure 51. Insulin staining in 7 μ m sections was quantified using Metamorph software. At least 50 islets were quantified for each pancreas in sections greater than 200 μ m apart. *: P<0.05, **: P<0.01.

The increase in β cell mass was further validated by measuring the total insulin content of transgenic and wild-type mice. The total insulin content was also significantly increased in transgenic mice over-expressing Tmem27 (Figure 53). To rule out that increased insulin resistance was responsible for the observed

increase in β cell mass I performed insulin-tolerance tests (ITT). No difference in glucose clearance following a bolus insulin injection was observed (Figure 54).

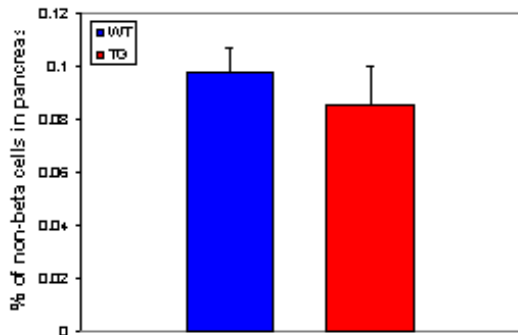


Figure 52. Quantification of non- β cells of islets was performed by immunostaining with a cocktail consisting of anti-glucagon, somatostatin and pancreatic polypeptide antibodies. Analysis was carried out as in Fig. 51.

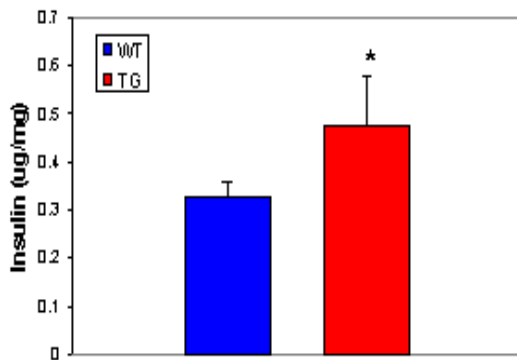


Figure 53. Whole pancreata from transgenic and wild-type mice ($n = 5$) were isolated and homogenized in acid/ethanol. Insulin content was normalized per pancreas weight. *: $P < 0.05$.

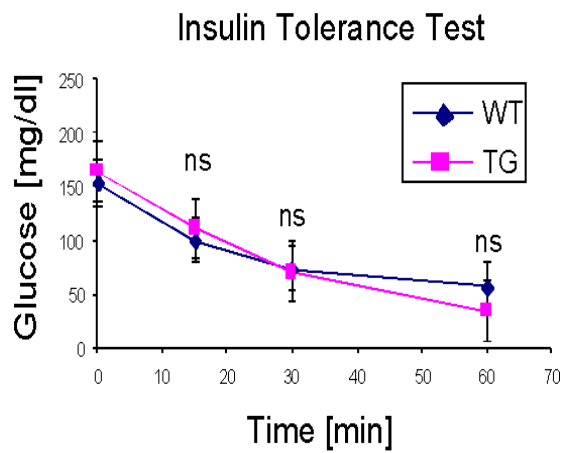


Figure 54. Insulin tolerance test performed on transgenic and littermate control mice. $N=6$ per genotype. Results were similar for both transgenic lines.

Furthermore, no significant difference in body weight, fasting insulin levels, plasma leptin concentrations and adiponectin levels were measured in transgenic mice compared control littermates (Figure 55). These data show that insulin resistance is not responsible for the increased β cell mass observed in the transgenic animals.

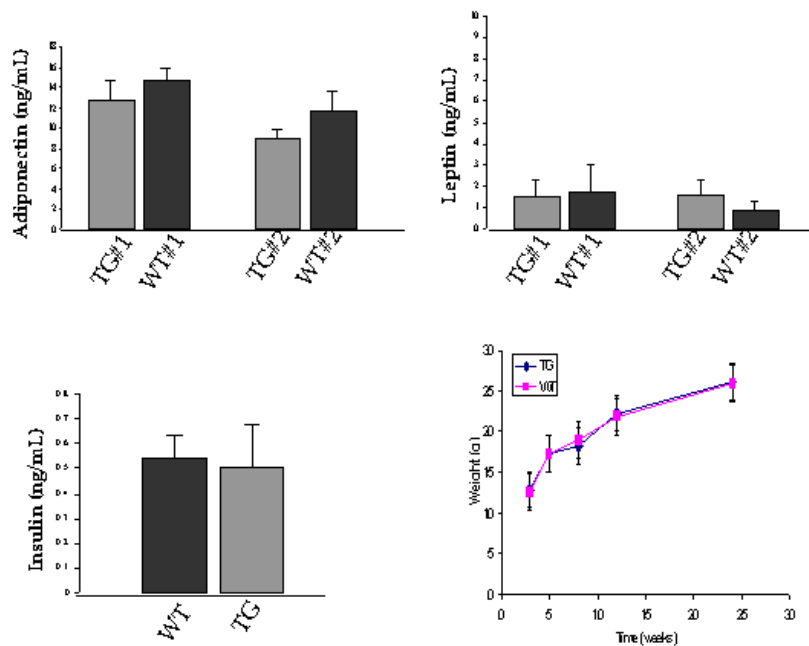


Figure 55. Adiponectin, leptin, and fasting insulin levels in plasma were measured in both transgenic lines and their littermate controls. Weight of transgenic mice along with controls were measured up to 6 months of age. There was no difference in either the metabolic parameters or the weight gain.

Increased β cell replication may lead to decreased glucose responsiveness due to dedifferentiation. Therefore, I performed glucose tolerance tests (IPGTT) and studied insulin secretion from islets that were isolated from either wild-type or

transgenic animals. Transgenic mice exhibited normal glucose tolerance (Figure 56) and I observed a robust ≈ 13 -fold increase in insulin secretion of islets isolated from transgenic mice in response to glucose stimulation, comparable to wild-type controls (Figure 57). Together, these data demonstrate that Tmem27 stimulates islet growth *in vivo* and that increased expression of Tmem27 does not impair regulated insulin secretion and glucose sensing.

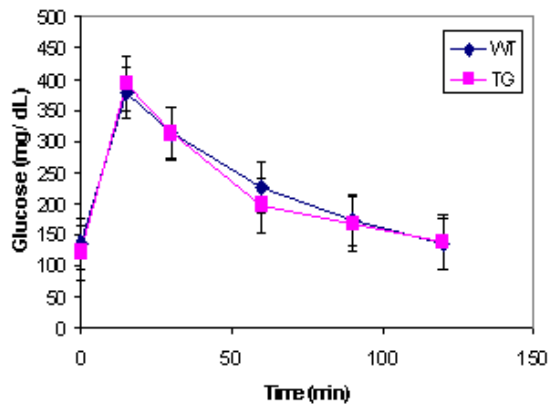


Figure 56. Intrapertoneal glucose tolerance test on transgenic and littermate control mice. N=6 per genotype. Results were similar for both transgenic lines.

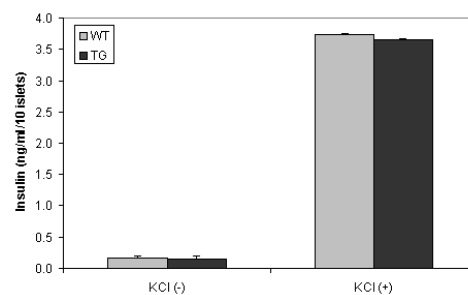
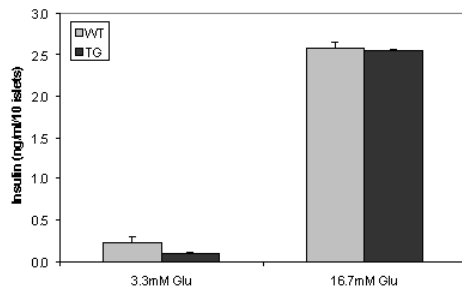


Figure 57. Insulin secretion of size-matched islets of transgenic mice and wild-type littermates in response to glucose and KCl.

Transgenic animals and their littermate controls were challenged with a high fat diet. Animals gained weight similarly and did not have a significant difference in fasting blood glucose levels. However, transgenic animals performed better in IPGTT showing that overexpression of Tmem27 in β cells was protective from the effects of the high fat diet (Figure 58).

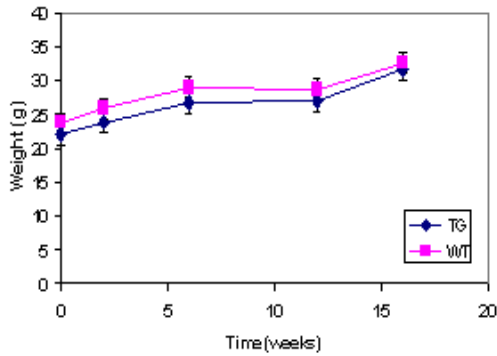
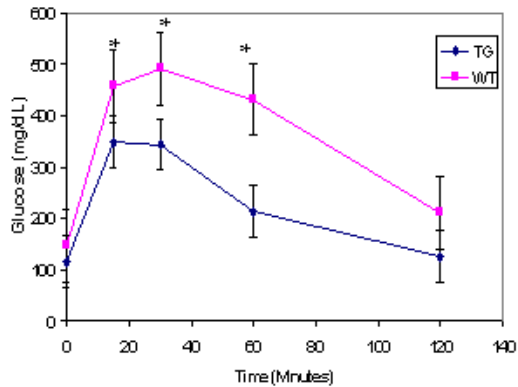


Figure 58. Transgenic mice and their littermate controls were fed a high fat diet over 16 weeks and their weight was monitored. There was no significant difference in weight gain between both sets of mice. N=6 per genotype.



Intraperitoneal glucose tolerance test on transgenic and littermate control mice. Glucose levels were significantly lower in transgenic mice. *: P < 0.05.

DISCUSSION

In this thesis a genomic approach was used to identify genes that may contribute to islet mass maintenance during adult life and islet growth following increased demand for insulin secretion. A number of transcription factors have been shown to be important regulators of both development and function of pancreatic β cells. TCF1 is a transcription factor that leads to progressive early-onset diabetes called MODY3 when mutated in humans. Experimental mouse models for MODY3, *Tcf1*^{-/-} and RIP-P291fsinsC, display decreased islet mass due to a progressive reduction in β cell number and proliferation rate. Expression profiles of islets isolated from *Tcf1*^{-/-} and wild-type littermate animals were compared in order to identify mitogenic factors that are regulated by Tcf1.

We found that *Tmem27* exhibits markedly reduced expression in the islets of diabetic *Tcf1*^{-/-} animals with decreased islet mass compared to wild-type littermates. Further experiments revealed that *Tmem27* is essential for optimal β cell growth in vitro and transgenic mice over-expressing *Tmem27* exhibit increased islet mass.

3.1 Tcf1 regulates expression of Tmem27

Promoter analysis and chromatin immunoprecipitation demonstrate that Tcf1 binds to conserved TCF1 binding sites in the *Tmem27* promoter and that it

activates transcription of this gene.

During the development of mouse kidney, *Tmem27* is detectable at day 13 of gestation in the ureteric bud branches. Its expression is progressively increased during later stages of the gestation extending into the neonatal periods and then is decreased in adult life (Zhang et al., 2001). Interestingly, we found normal levels of *Tmem27* mRNA in the kidneys of *Tcf1*^{-/-} animals (data not shown). *Tcf1* expression in adult kidneys is restricted to the proximal and distal tubules, whereas *Tcf2*, a related protein that can form heterodimers with *Tcf1* and shares 93%, 75% and 47% sequence identity in their DNA binding domains, dimerization domains, carboxyl-terminal activation domains, respectively, is mainly localized in the collecting ducts (Rey-Campos et al., 1991; Coffinier et al., 1999). *Tmem27* is specifically expressed in the collecting tubules and therefore overlaps in its expression with *Tcf2*, indicating that *Tcf2* homodimers may regulate the expression of *Tmem27* in these cells in the adult kidney. In pancreatic islets of *Tcf1*^{-/-} mice, *Tmem27* expression is profoundly reduced, indicating that *Tcf2* cannot substitute for *Tcf1*. This may be explained by different DNA binding specificities and/or by the higher *Tcf1* expression levels compared to *Tcf2* in pancreatic islets.

3.2 Expression of *Tmem27* in embryonic pancreas development

Tmem27 expression is found at the earliest stages of pancreatic

development (E10.5). Tmem27 is expressed in hormone-positive cells throughout development but becomes restricted to pancreatic β cells in the postnatal period. Tmem27 expression was not detected in Ngn3-positive neuroendocrine precursor cells. This expression pattern is reminiscent of the temporal and spatial expression of Pdx-1, an essential transcription factor for pancreas development, differentiation and insulin gene transcription (Jonsson et al., 1994; Offield et al., 1996; Ahlgren et al., 1998). Indeed, a conserved binding site of Pdx-1 was identified in the Tmem27 promoter that partially overlaps with the Tcf1 site and which exhibits binding activity in EMSA analysis (Figures 7 and 9), suggesting that Pdx-1 may also be a critical regulator of Tmem27. These data make it tempting to speculate that the membrane-bound or secreted form of Tmem27 contributes to the defect observed in Pdx-1 deficient mice, possibly by acting as a receptor or a signaling molecule (Jonsson et al., 2003).

3.3 Ectodomain shedding of Tmem27

I found that the N-terminal, extracellular domain of Tmem27 is cleaved and released from the plasma membrane of pancreatic β cells. Tmem27 does not co-localize with insulin granules or synaptic-like microvesicles, thereby ruling out the possibility that Tmem27 is released by the regulated secretory pathway. This is further supported by the observation that the cleaved protein cannot be detected in whole cell extracts of MIN6 cells and that release of the cleaved form

of Tmem27 is not regulated by glucose. Interestingly, cleavage of Tmem27 only occurs in pancreatic β cells and could not be detected in cells that were transfected with a Tmem27 expression vector. This may suggest that Tmem27 is cleaved by a β cell-specific or -enriched protease. However, reducing the expression of proteases that have known β cell-specific activity with siRNAs does not lead to any alterations in soluble Tmem27 levels. Biochemical data as well as siRNA experiments exclude the involvement of furin, PC1/3, PC2 and carboxypeptidase E.

PMA stimulated shedding of Tmem27 as well as inhibition of this induction by the hydroxamate-based compound BB94 suggests the involvement of the zinc-dependent metalloproteases of the metzincin family, which includes proteases containing a disintegrin and a metalloprotease (ADAM) domain. ADAMs have been shown to cleave a variety of substrates with important roles in development and disease, including cytokines, growth factors/receptors and adhesion molecules. In the pancreas, expression patterns are characterized for three members of this family. ADAM9, 10, and 17 are all expressed in the pancreatic anlagen. During development the expression of all three proteases gets restricted to different cell lineages. In the adult pancreas ADAM9 is only expressed in β cells whereas ADAM17 is expressed in all endocrine cell types. ADAM10 is detected in endocrine as well as exocrine pancreas (Asayesh et al.,

2005). ADAM9^{-/-} mice display no reduction in the release of soluble Tmem27 release from isolated islets excluding the role of this protease in cleavage. ADAM17^{-/-} mice are not viable, however, ADAM17^{ΔZn/ΔZn} mice, which lack the Zn²⁺ binding domain, live for 2-3 weeks and can be used for islet studies. A recent study also identified ADAM17 as a mediator of the regulated ectodomain shedding of ACE2 (Lambert et al., 2005). The cleavage site for ADAM17 mediated proteolysis of ACE2 is not clear, however, it is predicted to be in the juxtamembrane stalk region from the mass of the released peptide. The juxtamembrane regions of ACE2 and Tmem27 are highly homologous. Therefore, possible role of ADAM17 in Tmem27 shedding should be investigated with further studies in mice as well as with siRNA mediated targeting of ADAM17 expression in β cell lines.

Receptor shedding has been reported for members of diverse families of transmembrane receptors. For instance, the precursor form of hepatocyte growth factor is associated with the cell surface and biological function is dependent on proteolytic cleavage of an extracellular domain by the serine protease hepatocyte growth factor activator (HGFA)(Naldini et al., 1992; Miyazawa et al., 1993). Other receptors can bind to ligands upon cleavage and inhibit their activity. One example is the growth hormone-binding protein (GHBP), which derives from proteolytic shedding of the GH receptor (GHR) extracellular domain and is

complexed to a substantial fraction of circulating GH (Wang et al., 2002). Proteolytic shedding of receptors may not just release ligands or ligand binding proteins but can also be a means to regulate receptor function. For instance, one of the mechanisms that has evolved to modulate TNF function is the proteolytic cleavage of its cell surface receptors (Xanthoulea et al., 2004). The biological relevance is highlighted by identifications of mutations affecting shedding of the p55TNF receptor that have been linked with the development of the TNFR-associated periodic syndromes (McDermott, 2001). Our studies support a model by which the full length, membrane-bound form of Tmem27 is responsible for stimulating cell replication: i. Over-expression of full-length Tmem27 in β cell lines and non- β cells that do not cleave Tmem27 leads to increased cell replication, ii. Over-expression of a truncated form in β cells and non- β cells has no effect on cell replication, and iii. Conditioned media or co-culture experiments failed to provide evidence that the soluble form of Tmem27 stimulates cell replication. These studies indicate that identification of the cleavage enzyme that processes Tmem27 could be therapeutically used to develop drugs that inhibit the activity of this protease. Such an inhibitor may therefore reduce cleavage of Tmem27 and lead to constitutive receptor activation, thereby increasing β cell mass. The role of the extracellular, soluble form of Tmem27 is currently unknown and future studies need to establish if it serves as a ligand, a ligand-

binding protein or a receptor. However, its unique properties, including pancreatic β cell-specific and constitutive release, make it tempting to hypothesize that it may be exploited in the future as a biomarker for islet mass if sensitive RIAs or ELISAs can be developed to detect this protein in serum samples.

3.4 Tmem27 influences insulin secretion

In MIN6 cells overexpression of Tmem27 leads to a decrease in insulin secretion while electroporation of cells with si-Tmem27 increases insulin secretion. These data contradict recent findings by Fukui et al. that show Tmem27 augments insulin secretion in INS1 cells through its interaction with the SNARE complex. I failed to detect this interaction through immunoprecipitation of Tmem27 from MIN6 cells. I further show immunofluorescence data that refute interaction of Tmem27 with VAMP-2 and syntaxin-1, components of the SNARE complex. Additional experiments are necessary to illuminate the cause for the differences in both sets of data, however, one explanation may be the different expression levels of Tmem27. When I electroporate MIN6 cells with either pTmem27 or si-Tmem27, western blots show marked increase or decrease in protein levels. Representative immunoblots in the Fukui et al. show less robust regulation of Tmem27 in INS1 cells. Thus levels of protein expression may specify thresholds for Tmem27 function. This hypothesis may also explain

the lack of islet hypertrophy in RIP-Tmem27 transgenic mice generated by Fukui et al. The Tmem27 protein levels display slight increase in islets of transgenic animals compared to wild-type controls. Another major difference between the two studies is the β cell lines that are used to measure insulin secretion. All my experiments were done in MIN6 cells that were transiently transfected whereas Fukui et al. used INS1 cells that stably overexpress Tmem27. It is possible to postulate that long-term overexpression of Tmem27 may affect cell lines differently. Moreover, I show that endogenous Tmem27 does not co-localize with SNARE complex proteins with immunofluorescence on primary islets, which is a more physiologically relevant approach than INS1 cells that are clonally selected.

3.5 Tmem27 stimulates β cell growth in vivo

In this study I have also established that Tmem27 controls islet growth *in vivo*. The expression of Tmem27 is reduced in *Tcf-1^{-/-}* mice and increased in three animal models of islet hypertrophy: *ob/ob*, *db/db* and *aP2-Srebp-1c* transgenic mice. I also show that expression of Tmem27 is correlated with islet mass in the BKS-Lepr/J mice. It is interesting that expression of Tmem27 is also increased in the hypertrophic kidneys after renal ablation, indicating that it may play a role in compensatory growth responses to organ injury (Zhang et al., 2001). Significantly, two independent lines of transgenic mice with increased expression

of Tmem27 in pancreatic β cells exhibited a \approx 2-fold increase in pancreatic islet mass and insulin content. Over-expression of Tmem27 in β cells had no effect on non- β cell mass, further supporting the notion that the full-length, membrane bound form is responsible for stimulating cell growth. Although under normal a chow fed diet I did not observe alterations of glucose homeostasis, increased β cell mass together with unaltered glucose sensing would likely be beneficial in insulin resistance states. Thus I challenged the transgenic animals and their littermates with a high fat diet. The high fat diet did not lead to any differences in weight gain or fasting glucose levels between the two sets of mice. However, intraperitoneal glucose tolerance tests show that transgenic animals are more glucose responsive than their littermates. Future studies with loss-of-function and gain-of-function mutations will further elucidate the role of Tmem27 in the maintenance of islet mass and insulin secretion.

Adult pancreatic β cells retain a significant proliferative capacity as islet mass is adaptable to metabolic demand in the body. β cell proliferation is controlled by the cell cycle molecular machinery. The earliest account of β cell mass regulation by cell cycle alterations came from studies in transgenic mice overexpressing SV40 large T-antigen in the β cell. These mice displayed increased β cell replication, islet hyperplasia, and consequently insulinomas (Hanahan, 1985). SV40 large T-antigen promotes proliferation by inactivating

p53 as well as the retinoblastoma tumor suppressor protein (pRb), both important in the G1 checkpoint of the cell cycle (Sherr, 2000; Levine, 1997). Supporting data for the importance of G1 checkpoint in β cell proliferation was obtained from cdk-4 deficient mice that display β cell hypoplasia causing neonatal diabetes (Rane et al., 1999). Moreover, a knocked-in constitutively active cdk-4 allele results in beta cell hyperplasia. D-cyclins are also key regulators of G1 phase. Two members of this family, cyclin D1 and cyclin D2, have been shown to be important in β cell replication and growth (Zhang et al., 2005; Georgia and Bhushan, 2004). I investigated whether increase in cell replication caused by Tmem27 expression was mediated by cdk-4 or cyclin D1. I checked the levels of each protein in western blots 48 hours after MIN6 cells were transfected with an expression vector of Tmem27. I could not detect a difference in the expression levels of either protein (data not shown).

A number of growth factors have been identified as capable of increasing β cell replication including lactogens, insulin, insulin-like growth factors (IGFs), hepatocyte growth factor (HGF), and glucagon-like peptide-1 (GLP-1).

Lactogens include placental lactogen (PL), prolactin (PRL), and growth hormone (GH). Role of lactogens in regulation of β cell mass and function has been studied extensively during pregnancy. PL and PRL signal through a common PRL receptor (PRLR). Both PRLR and GH receptor (GHR) belong to the

cytokine family of receptors that interact with members of the Janus Kinase (JAK) family of tyrosine kinases (Bole-Feysot et al., 1998). JAKs, upon phosphorylation, bind to members of the Signal Transduction and Activators of Transcription (STAT) family of transcription factors, which then translocate to the nucleus and activate expression of genes. Recent studies indicate that β cell replication induced through the PRLR is dependent on the activation of JAK2/STAT5 signalling pathway that results in the modulation of cyclin D2 expression (Friedrichsen et al., 2001 and 2003).

Insulin, IGF-I and IGF-II all have been shown to be important for growth and cell proliferation during embryogenesis and adult life. Insulin and IGF-I bind to tyrosine kinase receptors called insulin receptor (IR) and IGF-I receptor (IGF-IR), respectively. IGF-II can bind to both receptors. In vitro data obtained from β cell lines as well as isolated islets demonstrated that IGF-I and IGF-II increased β cell replication. IGF-I most likely leads to the activation of Erk1/2, phosphoinositide 3 (PI3)-kinase and subsequently mTOR/p70(S6K) signaling pathways through the insulin receptor substrate (IRS)-2 (Lingohr et al., 2002).

In vitro studies and transgenic mice overexpressing HGF in β cells suggest that HGF might be important for β cell proliferative response during insulin resistance, obesity, and partial pancreatectomy. HGF binds with high affinity and activates the transmembrane receptor encoded by the c-met protooncogene

(Furge et al., 2000). In the β cell line INS-1, HGF-induced cell replication involves signaling through PI3 kinase and atypical PKCs (Gahr et al., 2002). However, conditional knockout mice with disrupted HGF/c-met signaling in β cells display normal β cell mass and proliferation suggesting that HGF is not essential for normal β cell growth and proliferation (Roccisana et al., 2005).

In addition to the lactogens produced during pregnancy, the only well characterized stimulant for beta cell growth in a physiological situation is the gastrointestinal incretin hormone GLP-1. GLP-1 binds to the seven-transmembrane-spanning G protein-coupled receptor GLP-1R and has been shown to control blood glucose levels by stimulating insulin secretion, insulin biosynthesis, β cell proliferation and by inhibition of gastric emptying and glucagon release (Drucker, 2006). GLP-1 stimulated β cell proliferation in studies using isolated islets and β cell lines appears to involve activation of genes such as c-jun, junD, nur77 and c-fos (Buteau et al., 2001; Susini et al., 1998). These studies and others also implicate the involvement of signaling molecules such as PI3 kinase, Akt/PKB and PKC ζ (Buteau et al., 1999; Wang et al., 2004; Buteau et al., 2001).

Recent evidence emphasizes the importance of PI3 kinase and Akt signaling in regulation of β cell mass as various growth factors has been shown to activate these molecules. In β cells, the molecules and mechanisms that

mediate Akt signaling is not well defined. However, *in vivo* and *in vitro* experiments suggest that Akt could mediate proliferative signals induced by activation of Irs-2 (White, 2002). One of the mechanisms used for cell cycle regulation by Akt is inhibition of glycogen synthase kinase 3 β (GSK3 β) by phosphorylation. This inhibition leads to cyclin D1 and c-Myc accumulation in the nucleus and reduced levels of the cell cycle inhibitor p21^{CIP} (Chang et al., 2003). Akt has also been shown to regulate cell cycle by inactivation of the Foxo family of transcription factors (Martinez-Gac et al., 2004). Overexpression of Foxo transcription factors causes inhibition of cell proliferation (Chang et al., 2003). Moreover, decreased levels of Foxo1 restore Pdx1 expression and β cell proliferation in mice deficient in Irs-2, suggesting that Akt induced proliferative signals can be mediated by Foxo1 and Pdx1 (Kitamura et al., 2002).

It will be important to elucidate the exact molecular mechanisms Tmem27 utilizes in order to regulate cell replication. Tmem27 might exert its effects through one of the pathways described above and further experiments are necessary in order to determine specific signaling events. Activation of previously described signaling molecules for growth such as JAK/STAT, Erk1/2, PI3 kinase, and Akt should be checked following Tmem27 expression. I did not find an increase in the expression levels of cell cycle modulators such as cdk-4 and cyclin D1 upon Tmem27 expression, however, control of cell cycle is very

complicated and requires a precise balance of many different proteins. Further experiments should be performed in order to distinguish which molecules mediate the growth effect of Tmem27.

3.6 Conclusion

In this thesis I have identified and characterized a novel growth factor in pancreatic β cells. I show that Tmem27 expression is directly regulated by Tcf1 elucidating a link between the mutated transcription factor and its consequent islet mass phenotype. I demonstrate that Tmem27 undergoes ectodomain shedding, however, the function of this process needs to be elucidated. The data collectively suggest that full-length Tmem27 is responsible for the proliferation response. Thus we speculate that release of the extracellular domain may be a signal used to regulate replication of β cells of the islet (Figure 59). Identification of the protease in control of Tmem27 shedding and the functional relevance of this cleavage is crucial. Such studies will validate Tmem27 or its inactivating protease as a novel pharmacological target for the treatment of diabetes.

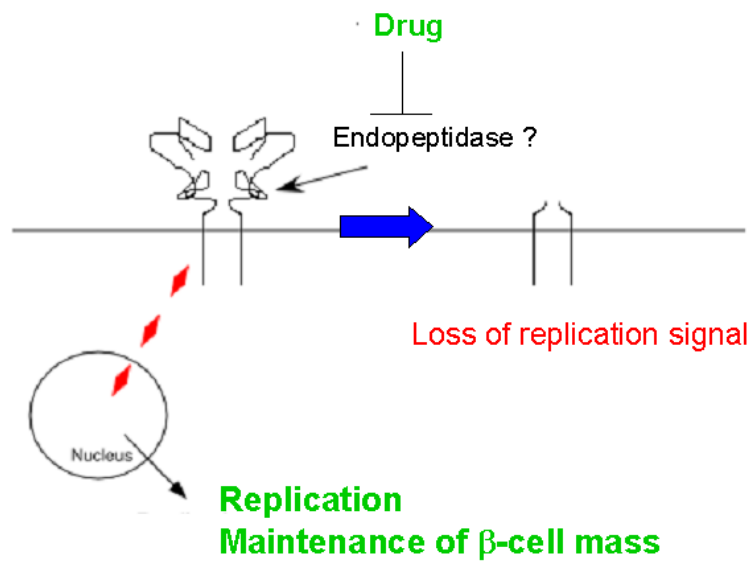


Figure 59. Model for Tmem27 function in β cells

EXPERIMENTAL PROCEDURES

Experimental animals

All animal models were housed in Laboratory of Animal Research Center (LARC), a pathogen-free animal facility at the Rockefeller University. The animals were maintained on a 12 hours light/dark cycle and fed a standard rodent chow. Genotyping of transgenic mice was performed on DNA isolated from 3 weeks old mice by PCR (Lee et al., 1998).

Vectors

The reporter plasmid pT27luc-wt was generated by cloning an 815-bp fragment of the mouse *Tmem27* promoter into pGL2-luciferase. The reporter plasmids pT27luc-m1 and -m2 are identical to pT27luc-wt except for mutated TCF1 binding sites at positions -56 to -59 and -116 to -119. Vector pTmem27.V5 is generated by cloning a PCR fragment of 696 bp that encompasses 30 bp of 5'UTR of *Tmem27* cDNA and the rest of the open reading frame except for the stop codon into pcDNA3.1/V5-His-TOPO vector from Invitrogen. Vector pTmem27-V5.del. was generated by deleting amino acid residues 17-129 of pTmem27.V5 vector using a PCR approach. The sequences of all constructs were confirmed by DNA sequencing.

Antibodies

Two peptides (anti-Tmem27N: VQSAIRKNNRNRINSAFFLD and anti-Tmem27C: GIPCDPLDMKGGHINDGFLT) were synthesized and processed to >90% purity, conjugated to KLH and used for immunization of rabbits (Bethyl Laboratories, Texas). Antisera were affinity purified and tested by western blotting and immunohistochemistry. Affinity purified antisera were used for all studies. Other antibodies used for immunoblotting and immunohistochemistry were obtained from the following sources: anti-insulin (Linco), anti-glucagon (Linco), anti-V5 (Invitrogen), anti-Tcf1 (Active Motif), anti-HA (Covance), anti-Glut2 (R&D Systems), anti-synaptophysin (Chemicon), anti-somatostatin (Cell Marque), anti-PP (Linco), and anti-Pdx1 (gift from Chris Wright). Rhodamine red conjugated donkey anti-guinea pig (Jackson Labs), Alexa 488 donkey anti-rabbit (Molecular Probes).

Cell culture

MIN6 cells were cultured with DMEM medium containing 25 mM glucose, 15% fetal bovine serum, and 5.5 μ M 2-mercaptoethanol. INS-1 cells were cultured with RPMI 1640 medium containing 11.1 mM glucose and 5% fetal bovine serum and 10 mM HEPES, pH7.4. HepG2 cells were cultured with DMEM medium containing 25 mM glucose and 10% fetal bovine serum. Pancreatic islets were

cultured in RPMI-1640 medium. S2 cells were cultured in Schneider's Medium with 10% FBS.

Transient transfections and luciferase assay

Fugene reagent (Roche) for HepG2 cells and Lipofectamine 2000 (Invitrogen) for MIN6 cells were used according to the manufacturer's directions in transient transfections. 0.5 µg of luciferase reporter construct, expression vector and CMV-LacZ were added per 35 mm dish. Luciferase was normalized for transfection efficiency by the corresponding β-galactosidase activity (Shih et al., 2001).

Crosslinking of proteins in cell lysates

MIN6 cells, grown to 90% confluency in 6 well plates, were harvested and resuspended in reaction buffer and reagent in 50 µl volume and incubated for 2 hrs at 4°C. Reactions were stopped by adding 50 mM Tris-HCl, pH 7.4 for 10 min on ice. Cells were then washed with PBS and lysed in RIPA buffer in the presence of protease inhibitors for 15 min at 4°C. Cell lysates were centrifuged for 5 min at 10,000 × g and the supernatants were subjected to reducing and non-reducing SDS-PAGE followed by immunoblotting. Crosslinking reagents and

buffers: BMH (Pierce) was dissolved in DMSO and incubated in PBS, and DTBP (Pierce) was dissolved in water and incubated in 0.2 M triethanolamine pH 8.0.

Inhibition and enzymatic cleavage of N-glycosylation

MIN6 cells that express pV5-TMEM27 were incubated with indicated concentrations of tunicamycin (Sigma) dissolved in DMSO and with DMSO alone for 12 h at 37°C. Cell lysates were then subjected to SDS-PAGE and immunoblotting with anti-V5 antibody.

Intact N-linked glycans were removed from secreted portion of TMEM27 with the recombinant enzyme N-glycanase (Prozyme, San Leandro, CA). Supernatants from MIN6 cells and pancreatic islets were denatured in 20 mM sodium phosphate pH 7.5, 0.1% SDS and 50 mM β -mercaptoethanol by heating at 100°C for 5 min. NP-40 was added to a final concentration of 0.75 % and reaction was incubated with N-glycanase for 3 h at 37°C.

Electrophoretic mobility shift assays (EMSA)

EMSA analysis was performed as described previously (Shih et al., 2001) with minor modifications. Assay was performed with 10 μ g of whole cell extracts in binding buffer (20 mM HEPES, pH 7.9, 10 % glycerol, 150 mM NaCl, 1 mM DTT). Whole cell extracts were incubated with ³²P-labeled double stranded

oligonucleotide probes containing the wildtype or mutant Tcf1 binding sites in the TMEM27 promoter (sequences: 5'-GGAGATTTTCGTAAATAACTGACA -3', 5'-GGGCGTTAATTATTAAACCTTTTA-3' and 5'-GGGCAGAGATTATTAACCTTTTA-3', respectively). Cold competitor was an unlabeled double-stranded oligonucleotide containing the Tcf1 binding site in the Fxr-1 promoter (sequence: 5'-GATGGGGGTTAATCAAGTAAACCACAC-3'). Supershifts were carried out with an anti-Tcf1 antibody (Geneka Biotechnology Inc., Montreal, Canada). ChIP analysis was carried out using isolated primary hepatocytes and isolated islets from C57/B6 mice or MIN6 cells, and the ChIP Assay kit (Upstate Cell Signaling Solutions, Lake Placid, NY) according to the manufacturers protocol. Tcf1 was precipitated with anti-HNF-1[©] antibody and DNA was amplified using primers sequences: 5'-ACAGGAGGCAGGTGGGAGGCTTCT -3' and 5'-CCCGGATTAGGGTATCGGAGAA -3'). Primers for apoM were 5'-GGGCTCAGCTTTCCTCCTA-3' and 5'-CTCCGCCTTAACTGTTCTCTGATG -3').

Whole Cell extract preparation

MIN6 cells were grown to 90% confluency in 150 mm tissue culture dishes. Cells were washed once in ice-cold PBS and scraped into 3 ml PBS. Cells were centrifuged at 4,000 x g for 4 min and resuspended in 2 volumes of high-salt extraction buffer (400 mM KCl, 20 mM Tris, pH 7.5, 20 % glycerol, 2 mM DTT, 1x

complete TM protease inhibitors (Boehringer Mannheim), and 20 µg/mL Aprotinin). Cell-lysis was performed by freezing and thawing, and the cellular debris was removed by centrifugation at 16,000 × g for 10 min at 4°C.

Pulse-Chase experiment with ³⁵S-labeled Tmem27

2 × 10⁵ MIN6 cells were plated in 35 mm dishes and incubated in methionine-free DMEM (DMEM-Met) for 70 min at 37°C. 200 µCi/mL of [³⁵S]methionine was added to DMEM-Met and cells were labeled in this media for 2 hours at 37°C. At the end of the pulse period, MIN6 cells were chased with complete growth medium for different periods. At the indicated time points, supernatants were collected and cells were lysed for immunoprecipitation. Cells were washed in ice cold PBS five times and scraped into PBS and centrifuged for 5 min at 2000 rpm. Cells were suspended in lysis buffer (20 mM Tris-HCl pH 7.4, 150 mM NaCl, 1% NP40, 1mM EDTA and protease inhibitors) and sonicated 5 sec for 4 times. 0.25% sodium deoxycholate was added to the samples, which were then mixed and incubated on ice for 15 min. Samples were centrifuged for 15 min at max speed at 4°C and the supernatant from the lysates were immuno-precipitated with α-Tmem27C for 16 hours at 4°C followed by incubation with Protein G-Sepharose for 1 hour. Collected MIN6 supernatants were adjusted to 20 mM Tris-HCl pH 7.4 and 1% NP40 along with protease inhibitors. α-Tmem27N

antibodies were used to immunoprecipitate cleaved protein for 16 hrs at 4°C followed by incubation with Protein G-Sepharose for 1 h. The sepharose beads were washed in ice-cold PBS 5-times for 5 min each and resuspended in SDS sample buffer (2% SDS, 62.5 mM Tris, pH 6.8). Samples were boiled for 5 min and supernatants were run on 4-15% gradient SDS gels. Gels were processed for autoradiography and exposed on film.

***In vitro* insulin secretion and hormone measurements**

Mouse islets were isolated and incubated in different glucose concentrations after an overnight culture. Insulin and glucagon were extracted from pancreata with acid ethanol (10% glacial acetic acid in absolute ethanol), sonicated for 10 min, and centrifuged 2 times at 4°C at 12,000xg for 10 min. Supernatants were collected and stored at -20°C for insulin and glucagon determinations by using sensitive RIA kits (Linco Research).

Pancreatic islet and RNA isolation

Pancreatic islets were isolated from 6 to 8 week-old mice. We used collagenase digestion and differential centrifugation through Ficoll gradients, with a modification of procedures previously described (Shih et al., 2002). Total RNA was then extracted using TRIzol reagent (Gibco-BRL) and following the

manufacturer's instructions. Contaminating genomic DNA was removed using 1 μ l of RNase free DNase-I (Boehringer) per 5 μ g of RNA.

Islet morphometry

The pancreata were fixed in paraformaldehyde and stained for insulin and pool of glucagon, pancreatic polypeptide and somatostatin as described above. Sections (7 μ m) through the entire pancreas were taken, and every sixth section was used for morphometric analysis. At least 288 non-overlapping images (pixel size 0.88 μ m) were scanned using a confocal laser-scanning microscope (Zeiss LSM 510, Germany). The parameters measured in this study were analyzed using integrated morphometry analysis tool in the Metamorph Software Package (Universal Imaging Corporation, PA). The area covered by cells stained by insulin or non- β cell pool was integrated using stained objects that are greater than 10 pixel in size.

RT-PCR

Total RNA was extracted using TRIZOL reagent (Invitrogen) and 10 μ g of RNA was treated with 5U of RNase-free DNase-I (Ambion). cDNA was synthesized using Moloney leukemia virus reverse transcriptase with dNTPs and random hexamer primers (Invitrogen). The cDNAs provided templates for PCRs using

specific primers in the presence of [32 P]dCTP and Taq polymerase as previously described (Shih et al., 2001). Quantitative PCR was performed using the Sequence Detection System 7700 (Applied Biosystems) for amplification and specific sequence detection. Forward and reverse PCR primers were used at a final concentration of 300 nM, and probes, containing a 5' fluorophor (6-FAM) and a 3' quencher (TAMRA), were used at a final concentration of 100 nM. Expression of Tmem27 was evaluated relative to the mRNA expression of the housekeeping gene α -actin in the same sample. Cycling parameters were: 2 min, 50°C; 10 min, 95°C; and 40 times: 30 s, 95°C; 1 min, 60°C. Primers and probes were purchased from Applied Biosystems.

Immunoblotting and Immunohistochemistry

Cytosolic protein extracts were separated by SDS-PAGE (4-15%) and transferred onto a nitrocellulose membrane (Schleicher & Schuell) by electroblotting. TMEM27 was detected with anti-Tmem27N and anti-Tmem27C antisera (1:500). Membranes were incubated with primary antibodies overnight at 4°C. Incubations containing the secondary antibody were performed at RT for 1 hr. SDS-PAGE under non-reducing conditions was performed under conditions omitting DTT from the sample buffer.

MIN6 cells were plated on coated slides (Nalge Nunc Int.) and fixed with 4% paraformaldehyde at 4°C for 20 min. Mouse islets were dissociated for 5 min at 37°C in the presence of 0.01% Trypsin-EDTA and were plated in collagen coated slides and fixed the same way. Slides were incubated in 0.01% saponin with 3% normal donkey serum in PBS for 30 min at room temperature and anti-Tmem27N and anti-Tmem27C (1:20) were added overnight at 4°C along with anti-insulin (1:600), anti-Glut2 (1:50), and anti-synaptophysin (1:500). Secondary antibodies were added for 30 min at RT.

Pancreata were fixed in 4% paraformaldehyde at 4°C for 4 h and embedded in paraffin. 7 µm sections were cut and after deparaffinization, antigen-unmasking was performed by microwaving slides in 0.01 M sodium citrate pH 6.0. Sections were permeabilized in 0.1 % Triton-X-100 and incubated in 3 % normal donkey serum in PBS for 30 min. Staining was completed as above.

Electron microscopy studies

MIN6 cells were fixed in 4% paraformaldehyde and 0.02% glutaraldehyde in 0.1 M cacodylate buffer, pH 7.4 for 2 hours. The cells were washed with PBS and embedded in 10% gelatin and refixed as above. Cell pellets were cryo-protected using a 2.3M sucrose solution in PBS, and samples were stored in liquid nitrogen until use (Griffith et al., 1983). Cryo, ultrathin sections were cut using glass

knives in a Reichert-Jung FC-4E cryo-ultramicrotome. The sections were collected on Formvar-carbon coated nickel grids, blocked with 1% BSA-PBS and incubated with anti-Tmem27C at a 1:10 dilution. Incubation was stopped by washing 2 times with PBS, 15 min each. The sections were then incubated with goat anti-rabbit IgG conjugated to 10 nm gold particles (Amersham Life Science, Arlington Heights, IL). The grids were processed and stained as described previously (Tokuyasu et al., 1973).

Thymidine incorporation studies

[³H]Thymidine incorporation in 5×10^4 cells/well in 24-well culture plates was assayed as follows. 48 hrs after electroporation, cells were incubated in growth arrest medium (0.5% FCS) for the next 24 hours and then incubated for an additional 24 hours in normal growth medium. For the last 4 h of the incubation, 0.25 μ Ci/well [³H]methylthymidine (Perkin Elmer) was added. After completion, cells were rinsed twice in ice-cold PBS, and incubated with 10% trichloroacetic acid (TCA) on ice for 20 min. After washing with 10% TCA, cells were solubilized in 0.2M NaOH/1% SDS for 10 min at room temperature. TCA-insoluble materials were neutralized with 0.2M HCl, and radioactivity was determined by a liquid scintillation counter.

RNA interference

Synthetic siRNAs were synthesized by Dharmacon Research (Lafayette, CO). siRNAs were designed for mouse TMEM27 ([NM_020626](#)) and Luciferase. The target sequences of siRNAs are: siTMEM27#1: gaagtacagtcggccataa, siTMEM27#2: ctacctatgctgatttaat. 3µg of each siRNA per 1 x 10⁶ cells were electroporated into MIN6 cells.

Generation of adenovirus

Adenovirus construct was generated by building a minigene with the addition of the intron between exon 1 and exon 2 to human Tmem27 cDNA. Sequence for 5' UTR, exon 1, intron 1, exon 2, and first 60 nucleotides of exon 3 were cloned into pcR11-TOPO (Invitrogen). This construct was digested with EarI and BstXI to obtain a 756 bp fragment and inserted into pcDNA3.V5 (BstXI and NotI) along with the 549 bp fragment taken out of Tmem27-pcDNA3.V5 with EarI and NotI. The minigene construct in pcDNA3.V5 was digested with HindIII and AvrII. The fragment was inserted into pCMV-Adenovirus vector digested with HindIII and SpeI to create Adv-hTmem27.

Generation of transgenic lines

Human Tmem27 cDNA was cloned next to 949 bp of the rat insulin promoter (RIP) in pcRII-TOPO vector (Invitrogen). Both transgenic lines were generated by pronuclear injection of the promoter and cDNA sequence that was extracted from the vector construct with NsiI. Transgenic lines are genotyped by southern blotting using AflII and NcoI that yields different patterns for both lines.

Bacterial protein production for monoclonal and polyclonal antibodies

Human Tmem27 sequence for amino acids 15-121 was subcloned into pGEX-4T-1 (Amersham) in frame with glutathione s-transferase (GST) including a cleavage site for thrombin. BL21 cells were transformed with construct and soluble protein was produced by inducing with 0.25 mM IPTG. Briefly, cultures were induced with IPTG when reached OD reading of 0.6 at A_{600} . Cultures were further incubated at 37 °C shaking for 5 hours. Bacteria was centrifuged at 6000 rpm for 10 min and dissolved in ice cold PBS that contains protease inhibitors (50 μ l PBS per 1 ml of culture). Solutions were sonicated at power 3 for 3 times 15 seconds each with a 1 minute cooling period between each pulse. Triton-X-100 was added to solutions to a concentration of 1% and tubes were rotated at 4°C for 30 minutes. Bacterial lysates are centrifuged at 25000 rpm for 25 min at 4°C and the supernatant is filtered with 45 μ m syringe filters. Supernatants were

incubated overnight at 4°C with GST-coupled beads and the next day beads were washed three times in ice cold PBS. The protein was eluted for ½ hr in 50 mM Tris pH 8.0, 10 mM reduced glutathione, and 5 mM β -octylglucoside. Eluted protein was dialyzed 16-24 hrs in 50 mM Tris pH 8.0 and concentrated in Microcon YM-3 centrifugal units.

S2 cell protein production for a polyclonal antibody

Sequence spanning amino acids 15 to 121 of human Tmem27 was cloned in frame to vector pMT/BiP/V5-His (Invitrogen) to create hTmem27-pMT/BiP/V5. S2 cells were transfected using CaPO₄ with hTmem27-pMT/BiP/V5 or GFP-pMT/BiP/V5. Briefly, S2 cells were seeded in 6 well plates (1.5 x 10⁶ cells in 3 ml) and transfected 24 hours later. Solution A was prepared by adding 36 μ l of 2M CaCl₂ and 19 μ g DNA to a total volume of 300 μ l with sterile water. Solution B was 300 μ l of 2x HEPES buffered saline (HBS). Solution A was added to solution B in a dropwise fashion while bubbling through with a pipette over 2 minutes. The mixed solution is incubated at room temperature for 45 minutes and added in drops while swirling the cells. In 24 hours, cells are centrifuged at 800 rpm for 10 minutes and washed twice with fresh medium. BiP is a secretion signal and hTmem27-V5 is secreted into the supernatant when S2 cells expressing hTmem27-pMT/BiP/V5 is induced with CuSO₄.

PCR-directed Mutagenesis

Two complementary oligonucleotides approximately 30 bps long were generated with the desired mutation in the middle of the sequence. PCR reaction was prepared with 125 ng of each primer and 50 ng DNA template. PCR conditions were as the following:

<u>Segment</u>	<u>Cycles</u>	<u>Temperature</u>	<u>Time</u>
1	1	95°C	30 sec
2	12	95°C	30 sec
		55°C	1 min
		68°C	6 min

Following cycling reaction was cooled to 37°C and digested with DpnI (20u) for 1 hour. 50 µl DH5α bacteria was transformed with 5 µl of digested PCR reaction and plated overnight for colony growth.

Protease Inhibitors

Inhibitor	Chemical Name
Pefabloc	[4-(2-Aminoethyl)benzenesulfonylfluoride HCl]
Aprotinin	
Leupeptin	Acetyl-Leu-Leu-Arg-al hydrochloride
PMSF	Phenylmethanesulfonyl fluoride
E64d	(2S,3S)- <i>trans</i> -Epoxy succinyl-L-leucylamido-3-methylbutane ethyl ester
Phosphoramidon	-(-Rhamnopyranosyloxyhydroxyphosphinyl)-Leu-Trp disodium salt
BB94	hydroxamic acid-type inhibitor

Statistical analysis

Results are given as mean \pm SD. Statistical analyses were performed by using a Student's *t*-test, and the null hypothesis was rejected at the 0.05 level.

REFERENCES

- Ahlgren, U., Jonsson, J., Edlund, H. 1996. The morphogenesis of the pancreatic mesenchyme is uncoupled from that of the pancreatic epithelium in IPF1/Pdx-1 deficient mice. *Development*. 122: 1409-16.
- Ahlgren, U., Pfaff, S.L., Jessell, T.M., Edlund, T., Edlund, H. 1997. Independent requirement for ISL1 in formation of pancreatic mesenchyme and islet cells. *Nature*. 385: 257-60.
- Ahlgren, U., Jonsson, J., Jonsson, L., Simu, K., Edlund, H. 1998. β -cell-specific inactivation of the mouse *Ipfl/Pdx1* gene results in loss of the beta-cell phenotype and maturity onset diabetes. *Genes. Dev.* 12: 1763-8.
- American Diabetes Association. Report of the expert committee on the diagnosis and classification of diabetes mellitus. 2001. *Diabetes Care*. 24: S5-20.
- Ang, S.L. and Rossant, J. 1994. HNF-3 beta is essential for node and notochord formation in mouse development. *Cell*. 78: 561-74.
- Apelqvist, A., Ahlgren, U., Edlund, H. 1997. Sonic hedgehog directs specialized mesoderm differentiation in the intestine and pancreas. *Curr. Biol.* 7: 801-4.
- Arribas, J. and Borroto, A. 2002. Protein ectodomain shedding. *Chem. Rev.* 102: 4627-38.
- Asayesh, A., Alanentalo, T., Khoo, N.K., Ahlgren, U. 2005. Developmental expression of metalloproteases ADAM 9, 10, and 17 becomes restricted to divergent pancreatic compartments. *Dev. Dyn.* 232: 1105-14.
- Black, R.A., Rauch, C.T., Kozlosky, C.J., Peschon, J.J., Slack, J.L., Wolfson, M.F., Castner, B.J., Stocking, K.L., Reddy, P., Srinivasan, S., Nelson, N., Boiani, N., Schooley, K.A., Gerhart, M., Davis, R., Fitzner, J.N., Johnson, R.S., Paxton, R.J., March, C.J., Cerretti, D.P. 1997. A metalloproteinase disintegrin that releases tumour-necrosis factor-alpha from cells. *Nature*. 385: 729-33.
- Bock, T., Pakkenberg, B., Buschard, K. 2003. Increased islet volume but unchanged islet number in ob/ob mice. *Diabetes*. 52; 1716-22.

- Bole-Feysot, C., Goffin, V., Edery, M., Binart, N., Kelly, P.A. 1998. Prolactin (PRL) and its receptor: Actions, signal transduction pathways and phenotypes observed in PRL receptor knockout mice. *Endocrine Reviews*. 19: 225-68.
- Bonner-Weir, S. 2000. Perspective: Postnatal pancreatic β cell growth. *Endocrinology* 141: 1926-29.
- Bort, R., Martinez-Barbera, J.P., Beddington, R.S., Zaret, K.S. 2004. Hex homeobox-gene dependent tissue positioning is required for the organogenesis of the ventral pancreas. *Development*. 131: 797-806.
- Buteau, J., Foisy, S., Rhodes, C.J., Carpenter, L., Biden, T.J., Prentki, M. 2001. Protein kinase C ζ activation mediates glucagon-like peptide-1-induced pancreatic beta-cell proliferation. *Diabetes*. 50: 2237-43.
- Buteau, J., Roduit, R., Susini, S., Prentki, M. 1999. Glucagon-like peptide-1 promotes DNA synthesis, activates phosphatidylinositol 3-kinase and increases transcription factor pancreatic and duodenal homeobox gene 1 (PDX-1) DNA binding activity in beta (INS-1)-cells. *Diabetologia*. 42: 856-64.
- Butler, A.E., Janson, J., Bonner-Weir, S., Ritzel, R., Rizza, R.A., Butler, P.C. 2003. β cell deficit and increased β cell apoptosis in humans with type 2 diabetes. *Diabetes*. 52: 102-110.
- Chang, F., Lee, J.T., Navolanic, P.M., Steelman, L.S., Shelton, J.G., Blalock, W.L., Franklin, R.A., McCubrey, J.A. 2003. Involvement of PI3K/Akt pathway in cell cycle progression, apoptosis, and neoplastic transformation: a target for cancer chemotherapy. *Leukemia*. 17: 590-603.
- Christesen, H.B., Jacobsen, B.B., Odili, S., Buettger, C., Cuesta-Munoz, A., Hansen, T., Brusgaard, K., Massa, O., Magnuson, M.A., Shiota, C., Matschinsky, F.M., Barbeti, F. 2002. The second activating glucokinase mutation (A456V): implications for glucose homeostasis and diabetes therapy. *Diabetes*. 51: 1240-6.
- Coffinier, C., Barra, J., Babinet, C., and Yaniv, M. 1999. Expression of the ν HNF1/HNF1beta homeoprotein gene during mouse organogenesis. *Mech. Dev*. 89: 211-3.
- Dor, Y., Brown, K., Martinez, O.I., Melton, D.A. 2004. Adult pancreatic β cells are formed by self-duplication rather than stem-cell differentiation. *Nature*. 429:41-6.

- Drucker, D.J. 2006. The biology of incretin hormones. *Cell Metab.* 3:153-65.
- Edlund, H. 2002. Pancreatic organogenesis-developmental mechanisms and implications for therapy. *Nat. Rev. Genet.* 3: 524-32.
- Fajans, S.S., Brown, M.B. 1993. Administration of sulfonylureas can increase glucose-induced insulin secretion for decades in patients with maturity-onset diabetes of the young. *Diabetes Care* 16: 1254-61.
- Finegood, D.T., Scaglia, L., Bonner-Weir, S. 1995. Dynamics of β cell mass in the growing rat pancreas. Estimation with a simple mathematical model. *Diabetes* 44; 249-56.
- Flier, S.N., Kulkarni, R.N., Kahn, C.R. 2001. Evidence for a circulating islet cell growth factor in insulin resistant states. *Proc. Natl. Acad. Sci. USA.* 98: 7475-80.
- Frayling, T.M., Evans, J.C., Bulman, M.P., Pearson, E., Allen, L., Owen, K., Bingham, C., Hannemann, M., Shepherd, M., Ellard, S., Hattersley, A.T. 2001. β cell genes and diabetes: molecular and clinical characterization of mutations in transcription factors. *Diabetes.* 50: S94-100.
- Friedrichsen, B.N., Galsgaard, E.D., Nielsen, J.H., Moldrup, A. 2001. Growth hormone- and prolactin-induced proliferation of insulinoma cells, INS-1, depends on activation of STAT5 (signal transducer and activator of transcription 5). *Mol Endocrinol.* 15:136-48.
- Friedrichsen, B.N., Richter, H.E., Hansen, J.A., Rhodes, C.J., Nielsen, J.H., Billestrup, N., Moldrup, A. 2003. Signal transducer and activator of transcription 5 activation is sufficient to drive transcriptional induction of cyclin D2 gene and proliferation of rat pancreatic beta-cells. *Mol Endocrinol.* 17:945-58.
- Froguel, P., Zouali, H., Vionnet, N., Velho, G., Vaxillaire, M., Sun, F., Lesage, S., Stoffel, M., Takeda, J., Passa, P., et al. 1993. Familial hyperglycemia due to mutations in glucokinase. Definition of a subtype of diabetes mellitus. *N. Eng.J. Med.* 328: 697-702.
- Fukui, K., Yang, Q., Cao, Y., Takahashi, N., Hatakeyama, H., Wang, H., Wada, J., Zhang, Y., Marselli, L., Nammo, T., Yoneda, K., Onishi, M., Higashiyama, S., Matsuzawa, Y., Gonzalez, F.J., Weir, G.C., Kasai, H., Shimomura, I., Miyagawa,

J., Wollheim, C.B., Yamagata, K. 2005. The HNF-1 target collectrin controls insulin exocytosis by SNARE complex formation. *Cell Metab.* 2: 373-84.

Furge, K.A., Zhang, Y.W., Vande Woude, G.F. 2000. Met receptor tyrosine kinase: enhanced signaling through adapter proteins. *Oncogene.* 19: 5582-9.

Gahr, S., Merger, M., Bollheimer, L.C., Hammerschmied, C.G., Scholmerich, J., Hugl, S.R. 2002. Hepatocyte growth factor stimulates proliferation of pancreatic beta-cells particularly in the presence of subphysiological glucose concentrations. *J Mol Endocrinol.* 28: 99-110.

Gapp, D.A., Leiter, E.H., Coleman, D.L. Schwizer, R.W. 1983. Temporal changes in pancreatic islet composition in C57BL/6J-db/db (diabetes) mice. *Diabetologia.* 25: 439-43.

Geisler, N., Schunemann, J., Weber, K. 1992. Chemical cross-linking indicates a staggered and antiparallel protofilament of desmin intermediate filaments and characterizes one higher-level complex between protofilaments. *Eur. J. Biochem.* 206: 841-52.

Georgia, S. and Bhushan, A. 2004. B cell replication is the primary mechanism for maintaining post-natal β cell mass. *Journal of Clin. Invest.* 114: 963-8.

Glaser, B., Kesavan, P., Heyman, M., Davis, E., Cuesta, A., Buchs, A., Stanley, C.A., Thornton, P.S., Permutt, M.A., Matschinsky, F.M., Herold, K.C. 1998. Familial hyperinsulinism caused by an activating glucokinase mutation. *N. Engl. J. Med.* 338: 226-30.

Gloyn, A.L., Noordam, K., Willemsen, M.A., Ellard, S., Lam, W.W., Campbell, I.W., Midgley, P., Shiota, C., Buettger, C., Magnuson, M.A., Matschinsky, F.M., Hattersley, A.T. 2003. Insights into the biochemical and genetic basis of glucokinase activation from naturally occurring hypoglycemia mutations. *Diabetes.* 52: 2433-40.

Gradwohl, G., Dierich, A., LeMeur, M., Guillemot, F. 2000. Neurogenin3 is required for the development of the four endocrine cell lineages of the pancreas. *Proc. Natl. Acad. Sci. USA.* 97: 1607-11.

- Grupe, A., Hultgren, B., Ryan, A., Ma, Y.H., Bauer, M., Stewart, T.A. 1995. Transgenic knockouts reveal a critical requirement for pancreatic beta cell glucokinase in maintaining glucose homeostasis. *Cell*. 83:69-78.
- Gu, G., Dubauskaite, J., Melton, D.A. 2002. Direct evidence for the pancreatic lineage: NGN3+ cells are islet progenitors and are distinct from duct progenitors. *Development*. 129: 2447-57.
- Habener, J.F., Kemp, D.M., Thomas, M.K. 2005. Minireview: Transcriptional regulation in pancreatic development. *Endocrinology*. 146: 1025-1034.
- Hagenfeldt-Johansson, K.A., Herrera, P.L., Wang, H., Gjinovci, A., Ishihara, H., Wollheim, C.B. 2001. Beta-cell-targeted expression of a dominant-negative hepatocyte nuclear factor-1 alpha induces a maturity-onset diabetes of the young (MODY)3-like phenotype in transgenic mice. *Endocrinology*. 142: 5311-20.
- Hanahan, D. 1985. Heritable formation of pancreatic beta-cell tumors in transgenic mice expressing recombinant insulin/simian virus 40 oncogenes. *Nature*. 315: 115-122.
- Hani, E.H., Stoffers, D.A., Chevre, J.C., Durand, E., Stanojevic, V., Dina, C., Habener, J.F., Froguel, P. 1999. Defective mutations in the insulin promoter factor-1 gene in late-onset type 2 diabetes mellitus. *J. Clin. Invest*. 104: R41-8.
- Herrera, P.L. 2000. Adult insulin and glucagons producing cells differentiate from two independent cell lineages. *Development*. 127: 2317-22.
- Jacquemin, P., Durviaux, S.M., Jensen, J., Godfraind, C., Gradwohl, G., Guillemot, F., Madsen, O.D., Carmeliet, P., Dewerchin, M., Collen, D., Rousseau, G.G., Lemaigre, F.P. 2000. Transcription factor hepatocyte nuclear factor 6 regulates pancreatic endocrine cell differentiation and controls expression of the proendocrine gene *ngn3*. *Mol. Cell Biol*. 20: 4445-54.
- Jonsson, J., Carlsson, L., Edlund, T., Edlund, H. 1994. Insulin-promoter-factor 1 is required for pancreas development in mice. *Nature*. 371: 606-9.
- Johnson, J.D., Ahmed, N.T., Luciani, D.S., Han, Z., Tran, H., Fujita, J., Mislser, S., Edlund, H., Polonsky, K.S. 2003. Increased islet apoptosis in *Pdx1*^{+/-} mice. *J. Clin. Invest*. 111: 1147-60.

- Kahn, C.R. 2003. Knockout mice challenge our concepts of glucose homeostasis and the pathogenesis of diabetes. *Exp. Diabetes Res.* 4: 169-82.
- Kawasaki, F., Matsuda, M., Kanda, Y., Inoue, H., Kaku, K. 2005. Structural and functional analysis of pancreatic islets preserved by pioglitazone in db/db mice. *Am. J. Physiol. Endocrinol. Metab.* 288: E510-8.
- Kitamura, T., Nakae, J., Kitamura, Y., Kido, Y., Wright, C.V., White, M.F., Arden, K.C., Accili, D. 2002. The forkhead transcription factor Foxo1 links insulin signaling to Pdx1 regulation of pancreatic beta cell growth. *J Clin Invest.* 110: 1839-47.
- Kloppel, G. 1985. Islet pathology and the pathogenesis of type 1 and type 2 diabetes mellitus revisited. *Surv. Synth. Pathol. Res.* 4: 110-25.
- Kulkarni, R.N., Otani, K., Baldwin, A.C., Kruetefeldt, J., Ueki, K., Stoffel, M., Kahn, C.R., Polonsky, K.S. 2004. Reduced β cell mass and altered glucose sensing impair insulin secretory function in β IRKO mice. *Am. J. Physiol. Endocrinol. Metab.* 286: E41-9.
- Lammert, E., Cleaver, O., Melton, D. 2003. Role of endothelial cells in early pancreas and liver development. *Mech. Dev.* 120: 59-64.
- Lee, C.S., De Leon, D.D., Kaestner, K.H., Stoffers, D.A. 2006. Regeneration of pancreatic islets after partial pancreatectomy in mice does not involve the reactivation of neurogenin3. *Diabetes.* 55: 269-72.
- Lee, Y.H., Sauer, B., Gonzalez, F.J. 1998. Laron dwarfism and non-insulin-dependent diabetes mellitus in the Hnf-1alpha knockout mouse. *Mol. Cell Biol.* 18: 3059-68.
- Levine, A.J. 1997. P53, the cellular gate keeper for growth division. *Cell.* 88: 323-31.
- Li, H., Arber, S., Jessell, T.M., Edlund, H. 1999. Selective agenesis of the dorsal pancreas in mice lacking homeobox gene Hlxb9. *Nat. Genet.* 23: 67-70.
- Lingohr, M.K., Buettner, R., Rhodes, C.J. 2002. Pancreatic β cell growth and survival – a role in obesity-linked type 2 diabetes? *Trends Mol. Med.* 8: 375-84.

- Macfarlane, W.M., Frayling, T.M., Ellard, S., Evans, J.C., Allen, L.I., Bulman, M.P., Ayres, S., Shepherd, M., Clark, P., Millward, A., Demaine, A., Wilkin, T., Docherty, K., Hattersley, A.T. 1999. Missense mutations in the insulin promoter factor-1 gene predispose to type 2 diabetes. *J. Clin. Invest.* 104: R33-9.
- Malecki, M.T., Jhala, U.S., Antonellis, A., Fields, L., Doria, A., Orban, T., Saad, M., Warram, J.H., Montminy, M., Krolewski, A.S. 1999. Mutations in NEUROD1 are associated with the development of type 2 diabetes mellitus. *Nat. Genet.* 23:323-8.
- Martinez-Gac, L., Alvarez, B., Garcia, Z., Marques, M., Arrizabalaga, M., Carrera, A.C. 2004. Phosphoinositide 3-kinase and Forkhead, a switch for cell division. *Biochem Soc Trans.* 32: 360-1.
- Marynissen, G., Aerts, L., Van Assche, F.A. 1983. The endocrine pancreas during pregnancy and lactation in the rat. *J. Dev. Physiol.* 5: 373-81.
- Matschinsky, F.M. 1990. Glucokinase as glucose sensor and metabolic signal generator in pancreatic β cells and hepatocytes. *Diabetes* 39:647-52.
- Miura, A., Yamagata, K., Kakei, M., Hatakeyama, H., Takahashi, N., Fukui, K., Nammo, T., Yoneda, K., Inoue, Y., Sladek, F.M., Magnuson, M.A., Kasai, H., Miyagawa, J., Gonzalez, F.J., Shimomura, I. 2006. Hepatocyte nuclear factor-4alpha is essential for glucose-stimulated insulin secretion by pancreatic β cells. *J. Biol. Chem.* 281: 5246-57.
- Naya, F.J., Huang, H.P., Qiu, Y., Mutoh, H., DeMayo, F.J., Leiter, A.B., Tsai, M.J. 1997. Diabetes, defective pancreatic morphogenesis, and abnormal enteroendocrine differentiation in BETA2/neuroD-deficient mice. *Genes Dev.* 11: 2323-34.
- Njolstad, P.R., Sovik, O., Cuesta-Munoz, A., et al. 2001. Neonatal diabetes mellitus due to complete glucokinase deficiency. *N. Engl. J. Med.* 344: 1588-92.
- Nishigori, H., Yamada, S., Kohama, T., Tomura, H., Sho, K., Horikawa, Y., Bell, G.I., Takeuchi, T., Takeda, J. 1998. Frameshift mutation, A263fsinsGG, in the hepatocyte nuclear factor-1beta gene associated with diabetes and renal dysfunction. *Diabetes.* 47: 1354-5.

- Odom, D.T., Zizlsperger, N., Gordon, D.B., Bell, G.W., Rinaldi, N.J., Murray, H.L., Volkert, T.L., Schreiber, J., Rolfe, P.A., Gifford, D.K., Fraenkel, E., Bell, G.I., Young, R.A. 2004. Control of pancreas and liver gene expression by HNF transcription factors. *Science*. 303:1378-81.
- Offield, M.F., Jetton, T.L., Labosky, P.A., Ray, M., Stein, R.W, Magnuson, M.A., Hogan, B.L., Wright, C.V. 1996. PDX-1 is required for pancreatic outgrowth and differentiation of the rostral duodenum. *Development*. 122: 983-95.
- Partis, M. D., Griffiths, D. G., Roberts, G. C., Beechey, R. B. 1983. Cross-linking of Multi Sub-unit Enzymes and Immobilization of Enzymes on Solid Supports *J. Protein Chem.* 2: 263.
- Pick, A., Clark, J., Kubstrup, C., Levisetti, M., Pugh, W., Bonner-weir, S., Polonsky, K.S. 1998. Role of apoptosis in failure of β cell mass compensation for insulin resistance and β cell defects in the male Zucker diabetic fatty rat. *Diabetes*. 47: 358-64.
- Pontoglio, M., Barra, J., Hadchouel, M., Doyen, A., Kress, C., Bach, J.P., Babinet, C., Yaniv, M. 1996. Hepatocyte nuclear factor 1 inactivation results in hepatic dysfunction, phenylketonuria, and renal Fanconi syndrome. *Cell*. 84: 575-85.
- Prado, C.L., Pugh-Bernard, A.E., Elghazi, L., Sosa-Pineda, B., Sussel, L. 2004. Ghrelin cells replace insulin producing β cells in two mouse models of pancreas development. *Proc. Natl. Acad. Sci. USA*. 101: 2924-9.
- Rane, S.G., Dubus, P., Mettus, R.V., Galbreath, E.J., Boden, G., Reddy, E.P., et al. (1999). Loss of Cdk4 expression causes insulin-deficient diabetes and Cdk4 activation results in beta-islet cell hyperplasia. *Nature Genetics*. 22, 44-52.
- Rey-Campos, J., Chouard, T., Yaniv, M., and Cereghini, S. 1991. vHNF1 is a homeoprotein that activates transcription and forms heterodimers with HNF1. *EMBO J*. 10: 1445-57.
- Richter, S., Shih, D.Q., Pearson, E.R., Wolfrum, C., Fajans, S.S., Hattersley, A.T., Stoffel, M. 2003. Regulation of apolipoprotein M gene expression by MODY3 gene hepatocyte nuclear factor-1alpha: haploinsufficiency is associated with reduced serum apolipoprotein M levels. *Diabetes*. 52: 2989-95.

Roccisana, J., Reddy, V., Vasavada, R.C., Gonzalez-Pertusa, J.A., Magnuson, M.A., Garcia-Ocana, A. 2005. Targeted inactivation of hepatocyte growth factor receptor c-met in beta-cells leads to defective insulin secretion and GLUT-2 downregulation without alteration of beta-cell mass. *Diabetes*. 54: 2090-102.

Sahin, U., Weskamp, G., Kelly, K., Zhou, H.M., Higashiyama, S., Peschon, J., Hartmann, D., Saftig, P., Blobel, C.P. 2004. Distinct roles for ADAM10 and ADAM17 in ectodomain shedding of six EGFR ligands. *J. Cell Biol.* 164: 769-79.

Sander, M., Neubuser, A., Kalamaras, J., Ee, H.C., Martin, G.R., German, M.S. 1997. Genetic analysis reveals that PAX6 is required for normal transcription of pancreatic hormone genes and islet development. *Genes Dev.* 11: 1662-73.

Sander, M., Sussel, L., Connors, J., Scheel, D., Kalamaras, J., Dela Cruz, F., Schwitzgebel, V., Hayes-Jordan, A., German, M. 2000. Homeobox gene Nkx6.1 lies downstream of Nkx2.2 in the major pathway of beta-cell formation in the pancreas. *Development*. 127: 5533-40.

Scaglia, L., Smith, F.E., Bonner-Weir, S. 1995. Apoptosis contributes to the involution of beta cell mass in the post partum rat pancreas. *Endocrinology*. 136: 5461-8.

Schlondorff, J. and Blobel, C.P. 1999. Metalloprotease-disintegrins: modular proteins capable of promoting cell-cell interactions and triggering signals by protein-ectodomain shedding. *J. Cell Sci.* 112: 3603-17.

Sherr, C.J. 2000. The Pezcoller lecture: Cancer cell cycles revisited. *Cancer Research*. 60: 3689-95.

Shih, D.Q., Bussen, M., Sehayek, E., Ananthanarayanan, M., Shneider, B.L., Suchy, F.J., Shefer, S., Bollileni, J.S., Gonzalez, F.J., Breslow, J.L., Stoffel, M. 2001a. Hepatocyte nuclear factor-1alpha is an essential regulator of bile acid and plasma cholesterol metabolism. *Nat. Genet.* 27:375-382.

Shih, D.Q., Screenan, S., Munoz, K.N., Philipson, L., Pontoglio, M., Yaniv, M., Polonsky, K.S., Stoffel, M. 2001b. Loss of HNF-1alpha function in mice leads to abnormal expression of genes involved in pancreatic islet development and metabolism. *Diabetes*. 50: 2472-80.

- Shih, D.Q., Stoffel, M. 2002. Molecular etiologies of MODY and other early-onset forms of diabetes. *Curr. Diab. Rep.* 2: 125-34.
- Shimomura, I., Hammer, R.E., Richardson, J.A., Ikemoto, S., Bashmakov, Y., Goldstein, J.L., Brown, M.S. 1998. Insulin resistance and diabetes mellitus in transgenic mice expressing nuclear SREBP-1c in adipose tissue: model for congenital generalized lipodystrophy. *Genes Dev.* 12: 3182-94.
- Slack, J.M.W. 1995. Developmental biology of the pancreas. *Development.* 121:1569-80.
- Sosa-Pineda, B., Chowdhury, K., Torres, M., Oliver, G., Gruss, P. 1997. The Pax4 gene is essential for differentiation of insulin-producing beta cells in the mammalian pancreas. *Nature.* 386: 399-402.
- Steiner, D.F. 1998. The proprotein convertases. *Curr. Opin. Chem. Biol.* 2: 31-9.
- Stoffel, M. and Duncan, S.A. 1997. The maturity-onset diabetes of the young (MODY1) transcription factor HNF4alpha regulates expression of genes required for glucose transport and metabolism. *Proc. Natl. Acad. Sci. USA.* 94:13209-14.
- Stoffers, D.A., Zinkin, N.T., Stanojevic, V., Clarke, W.L., Habener, J.F. 1997. Pancreatic agenesis attributable to a single nucleotide deletion in the human IPF1 gene coding sequence. *Nat. Genet.* 15: 106-10.
- Stoffers, D.A., Ferrer, J., Clarke, W.L., Habener, J.F. 1997b. Early-onset type-II diabetes mellitus (MODY4) linked to IPF1. *Nat. Genet.* 17:138-9.
- Stoffers, D.A., Stanojevic, V., Habener, J.F. 1998. Insulin promoter factor-1 gene mutation linked to early-onset type 2 diabetes mellitus directs expression of a dominant negative isoprotein. *J. Clin. Invest.* 102:232-41.
- Stride, A., Ellard, S., Clark, P., Shakespeare, L., Salzman, M., Shepherd, M., Hattersley, A.T. 2005. Beta-cell dysfunction, insulin sensitivity, and glycosuria precede diabetes in hepatocyte nuclear factor-1alpha mutation carriers. *Diabetes Care.* 28: 1751-6.

- Surmely, J.F., Guenat, E., Philippe, J., Dussoix, P., Schneiter, P., Temler, E., Vaxillaire, M., Froguel, P., Jequier, E., Tappy, L. 1998. Glucose utilization and production in patients with maturity-onset diabetes of the young caused by a mutation of the hepatocyte nuclear factor-1alpha gene. *Diabetes*. 47: 1459-63.
- Susini, S., Roche, E., Prentki, M., Schlegel, W. 1998. Glucose and glucocretin peptides synergize to induce c-fos, c-jun, junB, zif-268, and nur-77 gene expression in pancreatic beta(INS-1) cells. *FASEB J*. 12: 1173-82.
- Sussel, L., Kalamaras, J., Hartigan-O'Connor, D.J., Meneses, J.J., Pedersen, R.A., Rubenstein, J.L., German, M.S. 1998. Mice lacking the homeodomain transcription factor Nkx2.2 have diabetes due to arrested differentiation of pancreatic beta cells. *Development*. 125: 2213-21.
- Svenstrup, K., Skau, M., Pakkenberg, B., Buschard, K., Bock, T. 2002. Postnatal development of β cells in rats. Proposed explanatory model. *APMIS* 110; 372-8.
- Tomita, T., Doull, V., Pollock, H.G. Krizsan, D. 1992. Pancreatic islets of obese hyperglycemic mice (ob/ob). *Pancreas*. 7: 367-75.
- Topp, B.G., McArthur, M.D., Finegood, D.T. 2004. Metabolic adaptations to chronic glucose infusion in rats. *Diabetologia*. 47: 1602-10.
- Turner, A.J., Hooper, N.M. 2002. The angiotensin-converting enzyme gene family: genomics and pharmacology. *Trends Pharmacol. Sci*. 23: 177-83.
- Waechter, C.J., Lennarz, W.J. 1976. The role of polyprenol-linked sugars in glycoprotein synthesis. *Annu. Rev. Biochem*. 45: 95-112.
- Wang, H., Maechler, P., Hagenfeldt, K.A., Wollheim, C.B. 1998. Dominant-negative suppression of HNF-1alpha function results in defective insulin gene transcription and impaired metabolism-secretion coupling in a pancreatic beta-cell line. *EMBO J*. 17: 6701-13.
- Wang, H., Antinozzi, P.A., Hagenfeldt, K.A., Maechler, P., Wollheim, C.B. 2000. Molecular targets of a human HNF1 alpha mutation responsible for pancreatic beta-cell dysfunction. *EMBO J*. 19: 4257-64.

Wang, L., Coffinier, C., Thomas, M.K., Gresh, L., Eddu, G., Manor, T., Levitsky, L.L., Yaniv, M., Rhoads, D.B. 2004. Selective deletion of the Hnf1beta (MODY5) gene in beta-cells leads to altered gene expression and defective insulin release. *Endocrinology*. 145: 3941-9.

Wang, Q., Li, L., Xu, E., Wong, V., Rhodes, C., Brubaker, P.L. 2004. Glucagon-like peptide-1 regulates proliferation and apoptosis via activation of protein kinase B in pancreatic INS-1 beta cells. *Diabetologia*. 47: 478-87.

White, M.F. 2002. IRS proteins and the common path to diabetes. *Am J Physiol Endocrinol Metab*. 283: E413-22.

Wiedenmann, B., Rehm, H., Knierim, M., Becker, C.M. 1988. Fractionation of synaptophysin- containing vesicles from rat brain and cultured PC12 pheochromocytoma cells. *FEBS Lett*. 240: 71-77.

Wilson, M.E., Scheel, D., German, M.S. 2003. Gene expression cascades in pancreatic development. *Mech. Dev*. 120: 65-80.

Withers, D.J., Gutierrez, J.S., Towery, H., Burks, D.J., Ren, J.M., Previs, S., Zhang, J., Bernal, D., Pons, S., Shulman, G.I. et al. 1998. Disruption of IRS-2 causes type 2 diabetes in mice. *Nature*. 391: 900-4.

Wobser, H., Dussmann, H., Kogel, D., Wang, H., Reimertz, C., Wollheim, C.B., Byrne, M.M., Prehn, J.H. 2002. Dominant-negative suppression of HNF-1 alpha results in mitochondrial dysfunction, INS-1 cell apoptosis, and increased sensitivity to ceramide-, but not to high glucose-induced cell death. *J. Biol. Chem*. 277: 6413-21.

Yamagata, K., Yang, Q., Yamamoto, K., Iwahashi, H., Miyagawa, J., Okita, K., Yoshiuchi, I., Miyazaki, J., Noguchi, T., Nakajima, H., Namba, M., Hanafusa, T., Matsuzawa, Y. 1998. Mutation P291fsinsC in the transcription factor hepatocyte nuclear factor-1alpha is dominant negative. *Diabetes*. 47: 1231-5.

Yamagata, K., Nammo, T., Moriwaki, M., Ihara, A., Iizuka, K., Yang, Q., Satoh, T., Li, M., Uenaka, R., Okita, K., Iwahashi, H., Zhu, Q., Cao, Y., Imagawa, A., Tochino, Y., Hanafusa, T., Miyagawa, J., Matsuzawa, Y. 2002. Overexpression of dominant-negative mutant hepatocyte nuclear factor-1 alpha in pancreatic beta-cells causes abnormal islet architecture with decreased expression of E-cadherin, reduced beta-cell proliferation, and diabetes. *Diabetes*. 51: 114-23.

Yang, Q., Yamagata, K., Fukui, K., Cao, Y., Nammo, T., Iwahashi, H., Wang, H., Matsumura, I., Hanafusa, T., Bucala, R., Wollheim, C.B., Miyagawa, J., Matsuzawa, Y. 2002. Hepatocyte nuclear factor-1alpha modulates pancreatic beta-cell growth by regulating the expression of insulin-like growth factor-1 in INS-1 cells. *Diabetes*. 51: 1785-92.

Zimmet, P., Alberti, K.G., Shaw, J. 2001. Global and societal implications of the diabetes epidemic. *Nature*. 414: 782-7.

Zhang, H., Wada, J., Hida, K., Tsuchiyama, Y., Hiragushi, K., Shikata, K., Wang, H., Lin, S., Kanwar, Y.S., Makino, H. 2001. Collectrin, a collecting duct-specific transmembrane glycoprotein, is a novel homolog of ACE2 and is developmentally regulated in embryonic kidneys. *J. Biol. Chem*. 276: 17132-9.

Zhang, X., Gaspard, J.P., Mizukami, Y., Li, J., Graeme-Cook, F., Chung, D.C. 2005. Overexpression of cyclin D1 in pancreatic β cells in vivo results in islet hyperplasia without hypoglycemia. *Diabetes*. 54: 712-9.